small tilt carriers (β carriers) are centered on L, the relevant level being L_4; while the large-tilt carriers (α carriers) are probably located on the T-W line, close to T, and are holes. The similarity of the experimental results in arsenic and antimony suggests that the electron pockets found by Falicov and Golin at L should be identified with the β carriers. The relevant level would then be L_4 and the tilt angle would be small.

According to the results of Falicov and Lin, there are three β and six α ellipsoids in antimony, in agreement with experiment.[27] Assuming that in arsenic there are also three β ellipsoids, then the density of electrons is

$$n_\beta = (2m_0 E_F{}^\beta)^{3/2}/\pi^2\hbar^3[\beta_{11}(\beta_{22}\beta_{33}-\beta_{23}{}^2)]^{1/2}.$$

We find $n_\beta = 1.96\times10^{20}$ for the electron density.

[27] L. Windmiller and M. G. Priestley (to be published).

ACKNOWLEDGMENTS

We wish to thank J. Tait and R. Dryer for aid in crystal preparation. A discussion with L. R. Weisberg on his crystal-growth method is also acknowledged. The quartz bombs were made in the Argonne Optics and Glass shops and the advice of E. Yoder and J. Hodur is also acknowledged.

PHYSICAL REVIEW VOLUME 140, NUMBER 4A 15 NOVEMBER 1965

Effect of Applied Uniaxial Stresses on the Optical Absorption of *F* Centers in Alkali Halides*

STEPHEN EUGENE SCHNATTERLY†
Department of Physics, University of Illinois, Urbana, Illinois

The method of moments is used to analyze the effect of applied uniaxial stresses on the optical absorption of alkali halides containing F centers. By measuring the first-moment change of the F band due to uniaxial stresses applied in ⟨100⟩ and ⟨110⟩ directions, the coupling of the F-center excited state to lattice distortions of tetragonal and trigonal symmetry is evaluated. By measuring the third-moment change due to the same applied stresses, the separate contributions to the second moment of the F band of dynamic lattice distortions of tetragonal, trigonal, and breathing symmetries are evaluated. Measurements of the zeroth-moment change due to applied stresses allow evaluation of the validity of the Condon approximation. Calculations based on three simple models of the K band are compared with the results of a measurement of the change in zeroth and first moments of the K band produced by applied uniaxial stresses. The temperature dependence of the zeroth and first moments of the K band is calculated for the same three models. The results suggest that the K band is not due to transitions to a state of even parity.

I. INTRODUCTION

ONE of the most widely studied point defects in solids is the F center in alkali halides. The F center is a negative ion vacancy which has trapped an electron. The major optical transition associated with this defect, which occurs between an s-like ground state and a p-like excited state, produces a broad absorption band which is usually nearly Gaussian in shape with a half-width of about 0.2 eV at low temperatures.

Accompanying the F band on its high-energy side is a small absorption hump known as the K band, and to still higher energy, three smaller absorption bands known as the L_1, L_2, and L_3 bands. These bands have a peak absorption coefficient which is in constant proportion to that of the F band. This evidence suggests that the K and L bands are due to transitions to higher excited states of the F center.[1] Some work has been done in an effort to understand the nature of the states involved in the transitions. Mott and Gurney[2] have proposed that the K band is due to transitions to higher p-like states approaching the series limit at the conduction-band edge. Smith has calculated the K-band shape and oscillator strength expected in this case using a model potential well and finds approximate agreement with the observed K band.[3] Klick and Kabler have proposed a charge-transfer model for the L bands, in which the electron is transferred to a neighboring alkali ion, and the resulting atom raised to one of its excited states.[4] Wood has carried out a linear-combination-of-atomic-orbitals (*LCAO*) calculation for the F center in LiCl using $2s$ and $2p$ lithium functions out to the fifth-nearest neighbors.[5] His calculated energy levels are consistent with the observed absorption bands if one assumes that the K band is due to transitions to a state of even parity made partially allowed by odd-

* Work supported in part by a grant from the National Science Foundation.

† Based on a thesis submitted to the Department of Physics of the University of Illinois in partial fulfillment of requirements for the degree of Doctor of Philosophy in Physics.

[1] F. Lüty, Z. Physik **160**, 1 (1960).

[2] N. F. Mott and R. W. Gurney, *Electronic Processes in Ionic Crystals* (Dover Publications, Inc., New York, 1964), 2nd ed., p. 114.

[3] D. Y. Smith (private communication).

[4] C. C. Klick and M. N. Kabler, Phys. Rev. **131**, 1075 (1963).

[5] R. F. Wood, Phys. Rev. Letters **11**, 202 (1963).

parity lattice vibrations, and that the L_1 and L_2 bands correspond to linear combinations of p-like and f-like states, and the L_3 band to a p-like state.

Many studies of the optical properties of F centers in alkali halides have been carried out.[6] One of the most important characteristics of the F absorption band is the fact that the peak position of the band varies in a regular manner with the lattice constant. This variation is called the Ivey law[7] and can be written approximately,

$$E_{\max}=19.4a^{-1.88}\text{ eV},$$

where $E_{\max}$ is the photon energy at the peak of the band at liquid-nitrogen temperature, and a is the nearest-neighbor distance in angstrom units.

The Ivey law demonstrates that the peak position of the F band depends primarily on the lattice constant of the host crystal. Changes in the lattice constant, produced either by temperature variation[6,8] or applied hydrostatic pressure[8–10] cause changes in the peak position of the absorption band.

The most striking feature of the optical absorption bands of color centers is their breadth. The F-band half-width at low temperatures is typically 0.2 eV. This breadth is a result of the dynamic distortions of the lattice due to zero-point vibrations and phonons which perturb the energy levels involved in the electronic transition. The earliest attempt to calculate this broadening was that of Huang and Rhys.[11] They used a dielectric continuum approximation in which the coupling between the F-center electron and lattice vibrations was taken to be the interaction between the static charge distribution of the electron and the dipole field of the lattice waves. This interaction provides a linear coupling between the electronic energy and longitudinal optical modes of the lattice. The coupling strength can be calculated if the wave function of the F center in the ground and excited states is known. The Einstein approximation was made, all the optical modes being taken to have the same frequency ω_l.

The use of the continuum approximation with dipole-field coupling corresponds to neglecting the effect of distortions of the immediate environment on the energy levels of the trapped electron.

Huang and Rhys obtained good agreement with experimentally observed F-absorption band shapes.

Pekar[12] has carried the Huang-Rhys procedure one step further by solving for the wave functions of the states involved in the electronic transition and calculating the coupling of the states to the optical modes. A large number of parameters describing the optical properties of the F center were calculated, most of which are directly comparable with experimental results. Agreement is very good.

Lax generalized the Huang-Rhys-Pekar procedure to make an all quantum-mechanical calculation of the moments of the optical absorption band.[13] He assumed a linear coupling to the lattice modes, not specifying the mechanism of the interaction, nor restricting the calculation to modes of any particular branch of the phonon spectrum. In addition, he clarified the differences between the various approximations commonly made in dealing with absorption of light by impurities in crystals.

One of the most common approximations used, popular for its simplicity, is the quasimolecular approximation. Using this viewpoint, one describes the system in terms of a small number of suitably chosen parameters. Usually this description takes the form of a configuration-coordinate diagram. Lax has pointed out that although a system may be accurately described using such a model, the parameters chosen to fit the model to observed data may have no physical significance. For example, one may need to use a temperature-dependent mass to accurately fit the F center absorption or emission data with a configuration-coordinate model.

The work described in this paper involves measuring the effect of applied uniaxial stresses on the optical absorption of F centers in alkali halides. By applying uniaxial stresses along various crystallographic directions it is possible to measure the coupling of the F-center excited state to lattice distortions of various symmetries and to determine the extent to which dynamic lattice distortions of various symmetries contribute to the second moment of the unperturbed optical-absorption band. Section II presents a qualitative description of these effects. Section III summarizes the equations necessary for a quantitative interpretation of the experimental results using the method of moments. Section IV presents a discussion of the stress-induced dichroism to be expected in the K-band region on the basis of three simple models of the K band. Section V describes the experimental apparatus and method of data treatment. Section VI presents the experimental results with a discussion of their interpretation. The appendix describes a calculation of the temperature dependence of the optical absorption in the K-band region on the basis of three simple models of the K band.

II. QUALITATIVE DESCRIPTION OF THE EFFECT OF APPLIED UNIAXIAL STRESS ON THE OPTICAL ABSORPTION OF F CENTERS IN ALKALI HALIDES

A. The Coupling of the F-Center Excited State to Lattice Distortions of Specified Symmetries

When a stress is applied to a crystal containing F centers, the equilibrium positions of the ions shift,

[6] J. H. Schulman and W. D. Compton, *Color Centers in Solids* (Pergamon Press Inc., New York, 1962), p. 56.
[7] H. Ivey, Phys. Rev. **72**, 341 (1947).
[8] I. S. Jacobs, Phys. Rev. **93**, 993 (1954).
[9] W. G. Maisch and H. G. Drickamer, J. Phys. Chem. Solids **5**, 328 (1958).
[10] R. A. Eppler and H. G. Drickamer, J. Chem. Phys. **32**, 1418, 1734 (1960).
[11] K. Huang and A. Rhys, Proc. Roy. Soc. (London) **A204**, 406 (1950).
[12] S. I. Pekar, Zh. Eksperim. i Teor. Fiz. **20**, 510 (1950); **22**, 641 (1952).
[13] M. Lax, J. Chem. Phys. **20**, 1752 (1952).

thereby perturbing the electronic energy levels, and changing the absorption in the F-band region. By expressing the positions of the ions as linear combinations of normal coordinates, and applying uniaxial stresses in various directions, it is possible to obtain the coupling of the F-center excited electronic state to given normal coordinates. In most calculations involving lattice coordinates plane waves are chosen as the normal coordinates, since this representation takes advantage of the periodicity of the lattice. Near an F center, however, the lattice lacks periodicity, so plane waves lose their usual appeal. As viewed from the center of the vacancy, the lattice does, however, have cubic symmetry. It is advantageous, therefore, to classify the coordinates by their symmetry by specifying for which irreducible representation of the octahedral group they form a basis function. Henry, Schnatterly, and Slichter have shown that the F center ground state is not perturbed in first order by any lattice distortion, that the only normal coordinates which perturb the excited state in first order are those of Γ_1, Γ_3, and Γ_5 symmetry.[14] By applying a hydrostatic pressure, a lattice distortion of Γ_1 symmetry occurs and the coupling to that mode can therefore be measured. By applying uniaxial stresses in $\langle 100\rangle$ and $\langle 110\rangle$ directions, and measuring the difference in first moment of the band for light polarized parallel to and perpendicular to the stress, the coupling to modes of Γ_3 and Γ_5 symmetry, respectively, can be measured. These facts are proven in Ref. 14. Thus the coupling of the F-center excited state to long-wavelength acoustic distortions of Γ_1, Γ_3, and Γ_5 symmetry can be measured.

B. The Effect of Broadening Due to Dynamic Distortions of Specified Symmetries

The broadening of the F absorption band is produced by dynamic distortions of the lattice of the same three symmetries, but now short-wavelength phonons as well as optical-type phonons contribute. Figure 1 shows graphically the effect of a mode of each symmetry type on the p-like orbital triplet excited state of the F center. There are, of course, two degenerate modes of Γ_3 symmetry and three of Γ_5 symmetry. Figure 1 shows one example of each for simplicity. An evaluation of the contribution of each of the three symmetry modes to the total broadening of the band would be of great interest. A qualitative description of how this can be done will be given here. The results of a quantitative treatment are presented in Sec. III.

Consider the effect of applying an [001] stress to a sample containing F centers. This produces a static distortion of partly Γ_1 and partly Γ_3 symmetry. Figure 1(b) shows the effect of the Γ_3 part on the energy levels. Suppose the F band is broadened only by Γ_1 modes. Then the excited orbital triplet state remains degenerate

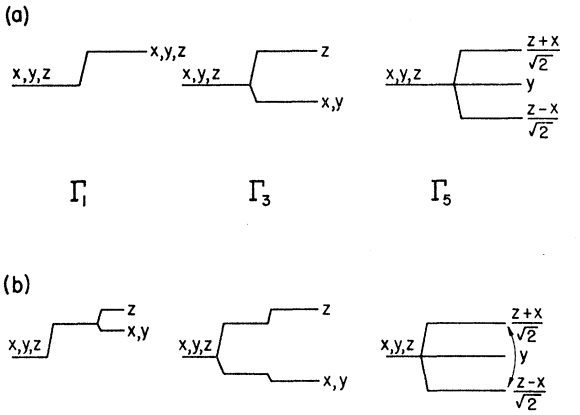

FIG. 1. (a) F-center excited state perturbed by lattice distortions of Γ_1, Γ_3, and Γ_5 symmetry. (b) F-center excited state perturbed by the above lattice distortions, and an additional distortion of Γ_3 symmetry.

until the stress is applied. If the band is broadened only by Γ_3 modes then the applied perturbation, being of the same symmetry, merely adds to the splitting produced by the dynamic distortions. If, on the other hand, the F band is broadened by Γ_5 modes, then the applied stress not only changes the energy levels, but also mixes the $z+x/\sqrt{2}$ state with the $z-x/\sqrt{2}$ state. Thus there are two cases. If the F band is broadened by Γ_1 and Γ_3 modes, the perturbation due to an applied static [001] stress can be simultaneously diagonalized with the dynamic perturbations (i.e., the Hamiltonians for the two perturbations commute) and so only energy-level changes occur. If Γ_5 modes broaden the F band, the applied perturbation cannot be simultaneously diagonalized with the Γ_5 dynamic perturbations and wave-function changes occur as well as energy-level changes.

Figure 2 shows the effect on the absorption band of

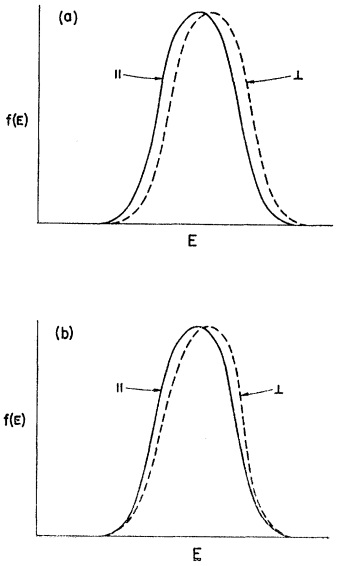

FIG. 2. (a) F absorption band shapes for light polarized parallel and perpendicular to an [001] stress for an F band broadened by Γ_1 and Γ_3 modes. (b) F absorption band shapes for light polarized parallel and perpendicular to an [001] stress for an F band broadened by Γ_5 modes.

[14] C. H. Henry, S. E. Schnatterly, and C. P. Slichter, Phys. Rev. **137**, A583 (1965).

the applied perturbation in each of the two cases. Figure 2(a) shows an F band broadened by Γ_1 and Γ_3 modes which has been perturbed with an applied [001] stress. The band is inhomogeneously broadened. Each F center in the crystal is perturbed as shown in the first two diagrams in Fig. 1(b). Therefore, the absorption band for light polarized parallel to the stress has been shifted rigidly to higher energy, while the band measured with light polarized perpendicular to the stress is shifted to lower energy. No change in band shape occurs. Figure 2(b) shows an F band broadened by Γ_5 modes, and perturbed by application of an [001] stress. Besides energy-level shifts, which are not shown, the wave function of the states on the high-energy side of the band are mixed with those on the low-energy side. The mixing is such as to increase the absorption for light polarized parallel to the stress on the high-energy side of the band, and decrease if for this polarization on the low-energy side. Qualitatively, this result is identical with that for broadening by Γ_1 and Γ_3 modes. Quantitatively, however, one might expect there to be a difference. The F band broadened by Γ_5 modes changes shape slightly upon being perturbed by application of an [001] stress. This change in shape can be used as a measure of the amount of broadening due to Γ_5 modes. Similarly, by applying a $\langle 110\rangle$ stress, it is possible to measure the amount of broadening due to Γ_3 modes.

Thus, by measuring the effect of a static stress on the optical absorption of F centers in alkali halides, it is possible not only to evaluate the coupling to the static lattice distortions produced by the stress, but also to obtain the contributions to the second moment of the unperturbed band made by dynamic lattice distortions of each symmetry.

III. METHOD OF MOMENTS APPLIED TO THE F CENTER

In most experiments in which the excited state of an atomic system is split or shifted, the effect of the applied perturbation is large enough compared with the line width that the energy-level changes can be measured directly. This is not the case for uniaxial stresses applied to a sample containing F centers in alkali halides. The ground state is an orbital singlet so there is no ground-state splitting which might produce a large population effect, and the half-width of the band at low temperatures is typically 0.2 eV, three orders of magnitude larger than the splittings of the excited state produced by attainable applied uniaxial stresses. Thus a method of analysis of the data is needed for the case in which the applied perturbation is small compared with the dynamic electron-lattice perturbations which are responsible for the linewidth.

Recently it was shown by Henry, Schnatterly, and Slichter[14] that a method appropriate to this case is the calculation and measurement of the moments of the optical absorption band, and the changes in moments produced by the applied perturbation. The changes in the first few moments resulting from the stress can be calculated very simply in terms of parameters of interest, such as the electron-lattice coupling to a lattice distortion of given symmetry, or the contributions to the second moment of the band of dynamic distortions of given symmetry. Measurements of the changes in these moments will therefore allow numerical evaluation of these parameters. A detailed derivation of the moment formulation is given in Ref. 14. Only the results that are pertinent to this work are given below.

Let us designate the excited state which gives rise to the F band by $|\beta\rangle$, and the linear coupling of this state to lattice mode $Q_{n\mu m}$ by $V_{n\mu m}$. $Q_{n\mu m}$ is the mth mode of symmetry $n\mu$ where n labels the irreducible representations of the octahedral group, and μ labels the basis functions of each representation. The second and third moments of the F band are due to the electron-lattice interaction and the spin-orbit interaction. They may be written

$$\langle E^2\rangle=\langle E^2\rangle_{\mathrm{EL}}+\langle E^2\rangle_{\mathrm{SO}}=\langle E^2\rangle_1+\langle E^2\rangle_3+\langle E^2\rangle_5+\tfrac{1}{2}\lambda^2, \quad (1)$$

$$\langle E^3\rangle=\langle E^3\rangle_{\mathrm{EL}}+\langle E^3\rangle_{\mathrm{SO}}=\langle E^3\rangle_1+\langle E^3\rangle_3+\langle E^3\rangle_5-\tfrac{1}{4}\lambda^3, \quad (2)$$

where $\langle E^i\rangle_n$ is the contribution to the ith moment of dynamic lattice distortions of symmetry Γ_n, and λ is the spin-orbit coupling constant defined in Ref. 14.

If lattice modes of only one frequency interact strongly with the F-center excited state, $\langle E^2\rangle_{\mathrm{EL}}$ and $\langle E^3\rangle_{\mathrm{EL}}$ can be written[15]

$$\langle E^2\rangle_{\mathrm{EL}}=\sum_{n\mu m\beta}\langle x|V_{n\mu m}|\beta\rangle^2\frac{h}{2M_{nm}\omega}\coth\frac{h\omega}{2kT}, \quad (3)$$

$$\langle E^3\rangle_{\mathrm{EL}}=\sum_{n\mu m\beta}\langle x|V_{n\mu m}|\beta\rangle^2\frac{h}{2M_{nm}\omega}(h\omega). \quad (4)$$

Consider the application of a hydrostatic pressure p to a sample containing F centers. The change in first moment $\langle\Delta E\rangle$ is found to be independent of the polarization and equal to

$$\langle\Delta E\rangle=p\langle a|\mathcal{A}_1|z\rangle. \quad (5)$$

Note the change in notation from $\langle z|A_1|z\rangle$ of Ref. 14 to $\langle z|\mathcal{A}_1|z\rangle$. If a uniaxial stress of magnitude $F_{[001]}$ is applied in the [001] direction, and light propagated in the [010] direction, the first moment change for light polarized parallel to and perpendicular to the stress is given by

$$\begin{aligned}\langle\Delta E_{\parallel}\rangle&=F_{3a}\langle z|\mathcal{A}_{3a}|z\rangle+F_1\langle z|\mathcal{A}_1|z\rangle\\&=\tfrac{2}{3}F_{[001]}\langle z|\mathcal{A}_{3a}|z\rangle+\tfrac{1}{3}F_{[001]}\langle z|\mathcal{A}_1|z\rangle, \quad (6)\\ \langle\Delta E_{\perp}\rangle&=\tfrac{2}{3}F_{[001]}\langle x|\mathcal{A}_{3a}|x\rangle+\tfrac{1}{3}F_{[001]}\langle z|\mathcal{A}_1|z\rangle\\&=-\tfrac{1}{3}F_{[001]}\langle z|\mathcal{A}_{3a}|z\rangle+\tfrac{1}{3}F_{[001]}\langle z|\mathcal{A}_1|z\rangle, \quad (7)\end{aligned}$$

so that

$$\langle\Delta E_{\parallel}\rangle-\langle\Delta E_{\perp}\rangle=F_{[001]}\langle z|\mathcal{A}_{3a}|z\rangle. \quad (8)$$

[15] C. H. Henry, thesis, University of Illinois, 1965 (unpublished).

If a uniaxial stress is applied in the [110] direction and light propagated in the [001] direction, the first-moment changes are

$$\langle\Delta E_{\parallel}\rangle=\tfrac{1}{2}F_{[110]}\langle x|\,\mathcal{A}_{5a}|y\rangle+\tfrac{1}{3}F_{[110]}\langle x|\,\mathcal{A}_1|x\rangle -\tfrac{1}{3}F_{[110]}\langle x|\,\mathcal{A}_{3a}|x\rangle, \quad (9)$$

$$\langle\Delta\rangle E_{\perp}=-\tfrac{1}{2}F_{[110]}\langle x|\,\mathcal{A}_{5a}|y\rangle+\tfrac{1}{3}F_{[110]}\langle x|\,\mathcal{A}_1|x\rangle -\tfrac{1}{3}F_{[110]}\langle x|\,\mathcal{A}_{3a}|x\rangle, \quad (10)$$

so that

$$\langle\Delta E_{\parallel}\rangle-\langle\Delta E_{\perp}\rangle=F_{[110]}\langle x|\,\mathcal{A}_{5a}|y\rangle. \quad (11)$$

The $\mathcal{A}_{m\mu}$ can be written as a constant times the μth basis function of the mth irreducible representation of the octahedral group. For example,

$$\mathcal{A}_{3a}=a_3(2z^2-x^2-y^2),$$
$$\mathcal{A}_{3b}=a_3\sqrt{3}(x^2-y^2).$$

The change in second moment produced by a stress involves only matrix elements of the $\mathcal{A}$'s, and will therefore give no new information. In addition, the change in $\langle E^2\rangle$ is extremely small, being second order in H_p, and would be difficult to measure.

The third moment change is linear in H_p and involves H_{SO} and H_{EL}. Information about H_{EL} and H_{SO} might therefore be obtained from its evaluation. Direct evaluation of $\langle\Delta E^3\rangle$ for applied uniaxial stresses in $\langle 100\rangle$ and $\langle 110\rangle$ directions results in

$$\langle\Delta E_{\parallel}{}^3\rangle-\langle\Delta E_{\perp}{}^3\rangle=3(\langle\Delta E_{\parallel}\rangle-\langle\Delta E_{\perp}\rangle) \times(\langle E_1{}^2\rangle+\langle E_3{}^2\rangle+\tfrac{1}{2}\langle E_5{}^2\rangle+\tfrac{1}{4}\lambda^2) \quad (12)$$

for a $\langle 100\rangle$ stress, and

$$\langle\Delta E_{\parallel}{}^3\rangle-\langle\Delta E_{\perp}{}^3\rangle=3(\langle\Delta E_{\parallel}\rangle-\langle\Delta E_{\perp}\rangle) \times(\langle E_1{}^2\rangle+\tfrac{1}{2}\langle E_3{}^2\rangle+\tfrac{5}{6}\langle E_5{}^2\rangle+\tfrac{1}{4}\lambda^2) \quad (13)$$

for a $\langle 110\rangle$ stress.

These changes can be compared with the third-moment changes that would result if the band rigidly shifts with no change in shape upon application of a stress. For the rigid-shift case, to first order in $\langle\Delta E_{\parallel}\rangle-\langle\Delta E_{\perp}\rangle$, the third moment change is

$$(\langle\Delta E_{\parallel}{}^3\rangle-\langle\Delta E_{\perp}{}^3\rangle)_{RS}=3(\langle\Delta E_{\parallel}\rangle-\langle\Delta E_{\perp}\rangle) \times(\langle E_1{}^2\rangle+\langle E_3{}^2\rangle+\langle E_5{}^2\rangle+\tfrac{1}{2}\lambda^2). \quad (14)$$

Hence for a $\langle 100\rangle$ stress

$$(\langle\Delta E_{\parallel}{}^3\rangle-\langle\Delta E_{\perp}{}^3\rangle)_{RS}-(\langle\Delta E_{\parallel}{}^3\rangle-\langle\Delta E_{\perp}{}^3\rangle)_{MEAS} =3(\langle\Delta E_{\parallel}\rangle-\langle\Delta E_{\perp}\rangle)(\tfrac{1}{2}\langle E_5{}^2\rangle+\tfrac{1}{4}\lambda^2) \quad (15)$$

and for a $\langle 110\rangle$ stress

$$(\langle\Delta E_{\parallel}{}^3\rangle-\langle\Delta E_{\perp}{}^3\rangle)_{RS}-(\langle\Delta E_{\parallel}{}^3\rangle-\langle\Delta E_{\perp}{}^3\rangle)_{MEAS} =3(\langle\Delta E_{\parallel}\rangle-\langle\Delta E_{\perp}\rangle)(\tfrac{1}{2}\langle E_3{}^2\rangle+\tfrac{1}{6}\langle E_5{}^2\rangle+\tfrac{1}{4}\lambda^2). \quad (16)$$

Since λ is known for many alkali halides from magneto-optic measurements, Eqs. (15) and (16) allow an evaluation of $\langle E_3{}^2\rangle$ and $\langle E_5{}^2\rangle$. If in addition, the total second moment of the band is measured, Eq. (1) allows $\langle E_1{}^2\rangle$ to be obtained.

IV. THE K BAND

A. Stress-Induced Dichroism for the Case of Nondegenerate Electronic States

The origin of the K band is not well understood. In an attempt to improve understanding of this absorption band, the stress-induced dichroism expected in the K-band region on the basis of three simple models will be calculated. It will be assumed that the K band is caused by transitions to a higher excited state of the F center. (See Sec. VI G.) We label the F-band ground and excited states by α and β, respectively, and the K state by γ. It was shown in Ref. 14 that a perturbation H_p mixes the nondegenerate states β and γ causing an exchange of area between the two bands of amount

$$\Delta A_{\eta\beta}=-\Delta A_{\eta\gamma} =2\sum_{\beta\gamma}\frac{\langle\alpha|P_\eta{}^\dagger|\beta\rangle\langle\beta|H_p|\gamma\rangle\langle\gamma|P_\eta|\alpha\rangle}{E_\beta{}^0-E_\gamma{}^0}, \quad (17)$$

where $E_\beta{}^0$ and $E_\gamma{}^0$ are the unperturbed energies of the β and γ states, respectively, and P_η is the electric-dipole operator for polarization η. This result is correct to first order in $H_p/(E_\beta{}^0-E_\gamma{}^0)$. In order to simplify the data analysis, it is necessary to assume that the change in area of each band occurs through a change in transition probability which is uniform throughout the band. That is,

$$\Delta f_\eta(E)=C_\eta f(E), \quad (18)$$

where C_η is given by

$$C_\eta=\Delta A_\eta/A \quad (19)$$

for each band.

In addition to exchanging area, each band will experience a first moment change. In analyzing the experimental results for the K band, the rigid shift approximation will be made. The change in absorption function for the rigid case is

$$\Delta f_\eta(E)=-(\partial f(E)/\partial E)\langle\Delta E_\eta\rangle \quad (20)$$

to first order in $\langle\Delta E_\eta\rangle$. Thus the change in absorption function in the K-band region is given by

$$\Delta f_\eta(E)=C_\eta f(E)-(\partial f(E)/\partial E)\langle\Delta E_\eta\rangle. \quad (21)$$

C_η is evaluated using Eqs. (17) and (19).

B. Evaluation for the s-State Model

By fitting the experimental data with Eq. (21), numerical values of C_η and $\langle\Delta E\rangle$ can be obtained. These can then be used to test the validity of a given model of the K band. For example, suppose that the K band is due to transitions to a Γ_1 (s-like) state which are made partially allowed by admixture of some Γ_{4u} F-band state. For an electron-lattice interaction H_{EL},

the K-state wave function can be written as[16]

$$|\gamma\rangle=|s\rangle\left\{1-\frac{1}{2}\sum_{\beta}\frac{|\langle\beta|H_{\mathrm{EL}}|s\rangle|^2}{\Delta^2}\right\}+\sum_{\beta}|\beta\rangle\frac{\langle\beta|H_{\mathrm{EL}}|s\rangle}{\Delta}$$
$$+\sum_{\beta}|\beta\rangle\frac{\langle\beta|H_{\mathrm{EL}}|s\rangle}{\Delta^2}\{\langle\beta|H_{\mathrm{EL}}|\beta\rangle-\langle s|H_{\mathrm{EL}}|s\rangle\}, \quad (22)$$

where $|\gamma\rangle$ denotes the K state and $\Delta=E_s-E_\beta$. Only lattice distortions of Γ_{4u} symmetry can couple the Γ_1 state to the Γ_{4u} state so the third term in Eq. (22) is zero. Combining Eqs. (17), (19), and (22),

$$C_\eta=\frac{2}{A_K\Delta}\sum_{\beta\gamma}\langle\beta|P_\eta^\dagger|\gamma\rangle\langle\gamma|H_p|\beta\rangle\langle\beta|P_\eta|\alpha\rangle$$
$$=\frac{2}{A_K\Delta}\sum_{\beta\beta'\beta''}\langle\alpha|P_\eta^\dagger|\beta\rangle\frac{\langle\beta|H_{\mathrm{EL}}|s\rangle}{\Delta}\frac{\langle s|H_{\mathrm{EL}}|\beta'\rangle}{\Delta}$$
$$\times\langle\beta'|H_p|\beta''\rangle\langle\beta''|P_\eta|\alpha\rangle. \quad (23)$$

By symmetry, $\langle\beta|H_{\mathrm{EL}}|s\rangle$ is independent of $|\beta\rangle$, so

$$C_\eta=\frac{2}{A_K}\frac{|\langle\beta|H_{\mathrm{EL}}|s\rangle|^2}{\Delta^2}\sum_{\beta\beta'\beta''}\langle\alpha|P_\eta^\dagger|\beta\rangle$$
$$\frac{\langle\beta'|H_p|\beta''\rangle}{\Delta}\langle\beta''|P_\eta|\alpha\rangle. \quad (24)$$

Consider an applied hydrostatic pressure. C_η is independent of the polarization of the light. For simplicity, light polarized in the z direction will be used.

$$C_z{}^p=\frac{2}{\Delta}\frac{A_F}{A_K}\frac{|\langle z|H_{\mathrm{EL}}|s\rangle|^2}{\Delta^2}\langle z|\mathfrak{A}_1|z\rangle p. \quad (25)$$

Since

$$\frac{A_K}{A_F}=\frac{|\langle z|H_{\mathrm{EL}}|s\rangle|^2}{\Delta^2} \quad (26)$$

it follows that

$$C_z{}^p=\frac{2}{\Delta}\langle z|\mathfrak{A}_1|z\rangle p. \quad (27)$$

By a similar analysis, it follows that for uniaxial stresses applied in the [001] and [110] directions

$$C_{11}-C_\perp=\frac{2}{\Delta}\langle z|\mathfrak{A}_{3a}|z\rangle F_{[001]}, \quad (28)$$

$$C_{11}-C_\perp=\frac{2}{\Delta}\langle x|\mathfrak{A}_{5a}|y\rangle F_{[110]}. \quad (29)$$

The first moment change of the K band due to the stress is

$$\langle\Delta E_\eta\rangle=\frac{1}{A_K}\sum_{\gamma\gamma'}\langle\alpha|P_\eta|\gamma\rangle\langle\gamma|H_p|\gamma'\rangle\langle\gamma'|P_\eta|\alpha\rangle \quad (30)$$
$$=\frac{1}{A_K}\sum_{\beta\beta'}\langle\alpha|P_\eta|\beta\rangle\frac{\langle\beta|H_{\mathrm{EL}}|s\rangle}{\Delta}\langle s|H_p|s\rangle$$
$$\times\frac{\langle s|H_{\mathrm{EL}}|\beta'\rangle}{\Delta}\langle\beta'|P_\eta|\alpha\rangle. \quad (30a)$$

So that for a hydrostatic pressure

$$\langle\Delta E\rangle_p=\langle s|\mathfrak{A}_1|s\rangle p. \quad (31)$$

For applied uniaxial stresses in $\langle100\rangle$ and $\langle110\rangle$ directions

$$\langle\Delta E\rangle_{11}-\langle\Delta E\rangle_\perp=0. \quad (32)$$

C. Evaluation for the d-State Model

Another possibility is that the K band is due to transitions to a d-like $(\Gamma_3+\Gamma_5)$ state which are made partially allowed by admixture of some Γ_4 F band state. In that case

$$|\gamma\rangle=|d\rangle\left(1-\frac{1}{2}\sum_{\beta}\frac{|\langle\beta|H_{\mathrm{EL}}|d\rangle|^2}{\Delta^2}\right)$$
$$+\sum_{\beta}|\beta\rangle\frac{\langle\beta|H_{\mathrm{EL}}|d\rangle}{\Delta} \quad (33)$$

to second order in H_{EL}. The calculation of C_η is similar to that given above and the result is the same, only in this case, A_K is given by

$$A_K=\sum_{\beta\beta' d}\langle\alpha|P_\eta|\beta\rangle\frac{\langle\beta|H_{\mathrm{EL}}|d\rangle}{\Delta}\frac{\langle d|H_{\mathrm{EL}}|\beta'\rangle}{\Delta}\langle\beta'|P_\eta|\alpha\rangle. \quad (34)$$

With this expression for A_K, Eqs. (27), (28), and (29) apply for the d-state model as well as the s-state model. The center of gravity shift of the K band is given by combining Eqs. (33) and (30):

$$\langle\Delta E_\eta\rangle=\frac{1}{A_K}\sum_{dd',\beta\beta'}\langle\alpha|P_\eta|\beta\rangle\frac{\langle\beta|H_{\mathrm{EL}}|d\rangle}{\Delta}\langle d|H_p|d'\rangle$$
$$\times\frac{\langle d'|H_{\mathrm{EL}}|\beta'\rangle}{\Delta}\langle\beta'|P_\eta|\alpha\rangle. \quad (35)$$

This sum will not be evaluated explicitly since it is a lengthy process, and the result is not particularly useful. The conclusion is that the d-state model predicts a polarization-dependent shift of the center of gravity of the K band due to applied uniaxial stresses. Thus,

$$\langle\Delta E\rangle_{11}-\langle\Delta E\rangle_\perp\neq0. \quad (36)$$

[16] L. I. Schiff, *Quantum Mechanics* (McGraw-Hill Book Company, Inc., New York, 1955), p. 154.

This can be seen by noting that $\langle\Delta E_\eta\rangle$ can be independent of the polarization of the light only if $\langle\beta|H_{\mathrm{EL}}|d\rangle$ be independent of $|\beta\rangle$ and $\langle d|H_p|d'\rangle$ be independent of $|d\rangle$, or $\langle d|H_p|d'\rangle$ be zero for the noncubic parts of H_p. Since neither is the case, $\langle\Delta E_\eta\rangle$ is not independent of the polarization.

D. Evaluation for the p-State Model

A third simple possibility is that the K band is due to transitions to a Γ_{4u} state. In this case

$$C_\eta=\frac{2}{A_K\Delta}\sum_{\beta\gamma}\langle\alpha|P_\eta^\dagger|\beta\rangle\langle\beta|H_p|\gamma\rangle\langle\gamma|P_\eta|\alpha\rangle. \quad (37)$$

For a hydrostatic pressure

$$C_z{}^p=\frac{2}{\Delta}\frac{\langle\alpha|P_z|\beta_z\rangle}{\langle\alpha|P_z|\gamma_z\rangle}\langle\beta_z|\,\mathfrak{A}_1|\gamma_z\rangle p$$
$$=\frac{2}{\Delta}\left(\frac{A_F}{A_K}\right)^{1/2}\langle\beta_z|\,\mathfrak{A}_1|\gamma_z\rangle p. \quad (38)$$

For [001] and [110] applied uniaxial stresses

$$(C_{11}-C_1)_{[001]}=\frac{2}{\Delta}(A_F/A_K)^{1/2}\langle\beta_z|\,\mathfrak{A}_{3a}|\gamma_z\rangle F_{[001]}, \quad (39)$$

$$(C_{11}-C_1)_{[110]}=\frac{2}{\Delta}(A_F/A_K)^{1/2}\langle\beta_x|\,\mathfrak{A}_{5a}|\gamma_y\rangle F_{[110]}. \quad (40)$$

The shift in the center of gravity due to applied stresses is similar to that for the F band. For applied hydrostatic pressure and [001] and [110] stresses

$$\langle\Delta E\rangle_p=\langle\gamma_z|\,\mathfrak{A}_1|\gamma_z\rangle p, \quad (41)$$

$$\langle\Delta E_{11}\rangle-\langle\Delta E_1\rangle=\langle\gamma_z|\,\mathfrak{A}_{3a}|\gamma_z\rangle F_{[001]}, \quad (42)$$

$$\langle\Delta E_{11}\rangle-\langle\Delta E_1\rangle=\langle\gamma_x|\,\mathfrak{A}_{5a}|\gamma_y\rangle F_{[110]}. \quad (43)$$

Analysis of experimental data will thus allow evaluation of the matrix elements of $\mathfrak{A}_1$, $\mathfrak{A}_3$, and $\mathfrak{A}_5$ between the F state and K state as well as the matrix elements of those operators in the K state.

It is desirable to generalize the above results to the case of a series of p-like states in order to derive results appropriate to the Mott and Gurney model.[2] The procedure described above applied directly to the case of a series of p-like states corresponds to assuming a constant value for

$$\langle\beta_i|\,\mathfrak{A}_{m\mu}|\gamma_j\rangle/A_p\Delta$$

in Eqs. (38)–(40) where A_p is the area of one of the p-like states, and assuming a constant value for the matrix elements of the $\mathfrak{A}$'s in Eqs. (41)–(43). This is not entirely realistic, since the matrix elements, energy denominator, and area of the absorption due to each p-like state can be expected to vary with position in the K band. In view of the large number of undetermined parameters, however, the only realistic approach available at the present time is to make the above assumptions. Equations (38)–(43) will therefore be used in analyzing the data for the Mott and Gurney model. They should provide average values of the above parameters over a limited interval of the K band.

V. EXPERIMENTAL PROCEDURE

A. Apparatus

The expressions which are to be evaluated are moment differences of the form

$$\langle\Delta E_{11}\rangle-\langle\Delta E_1\rangle=\frac{1}{A}\int(\Delta f_{11}(E)-\Delta f_1(E))EdE, \quad (44)$$

$$\langle\Delta E_{11}{}^3\rangle-\langle\Delta E_1{}^3\rangle=\frac{1}{A}\int(\Delta f_{11}(E)-\Delta f_1(E))(E-\bar{E})^3dE. \quad (45)$$

If $\Delta f_{11}(E)-\Delta f_1(E)$ is measured point by point through the F band, the above integrals can be numerically evaluated.

A method capable of measuring $\Delta f_{11}(E)-\Delta f_1(E)$ with high sensitivity was developed by Overhauser and Rüchardt[17] in 1958, in an attempt to measure the Stark effect of M and R centers in KCl. The same method was used in this measurement. A Bausch and Lomb monochromator adjusted to a bandpass of approximately 25 Å passes light through a Glan linear polarizer rotating at frequency ω. The light then passes through the sample in a direction perpendicular to the applied stress, and falls onto an RCA-7326 photomultiplier tube. The sample temperature was maintained at 80 ± 1°K for all measurements. The stress was applied to the crystal by a pivoted steel press which was connected to the bottom of the liquid-nitrogen reservoir by a bellows. The external forces were applied by hanging weights on a level arm which communicated to the press by a steel tube.

Before the stress is applied, the F centers in the sample absorb light independent of its polarization, so the intensity passing through the sample is constant in time. After the stress is applied, the absorption varies with polarization and the intensity is therefore modulated at frequency 2ω. A lock-in amplifier tuned to frequency 2ω amplifies the modulation which is a measure of $\Delta f_{11}(E)-\Delta f_1(E)$.

The F centers were produced by x irradiation at room temperature using an x-ray tube with a tungsten target operated at 100 KV constant potential and 25-ma filament current. The x-rays were filtered with 0.004-in. of copper foil to remove the low-energy photons from the beam. The samples were typically 12 mm×10 mm

[17] A. W. Overhauser and H. Rüchardt, Phys. Rev. **112**, 722 (1958).

$\times 3$ mm. The density of F centers is estimated to vary 30–50% from one surface of the sample to the other along the 3-mm thickness, due to absorption of x-rays by the crystal. This variation will not affect the results of the measurements as long as the applied stress is uniform.

For measurements in the F-band region, 20 min of x-ray time was required typically to produce an optical density of approximately two at the peak of the F band at nitrogen temperature. This corresponds to an F-center density of about 3×10^{16} cm^{-3}. The amount of absorption due to F-aggregate centers and V-type centers produced by this treatment was very small.

The K-band measurements required much larger x-ray exposures (10–12 h) and a significant amount of absorption due to other centers was produced in this case. This is one of the possible causes of systematic errors in K-band measurements.

Representative measurements for the F band were also made on KBr:KH crystals which were x-irradiated at room temperature for 15 sec to produce the F centers. The concentration of F-aggregate centers and V-type centers was negligible for these crystals.

The sensitivity of this measurement was limited by a noise level of approximately

$$\left(\frac{\Delta I}{I}\right)_{\text{noise}} \simeq 5\times10^{-5}, \tag{46}$$

where I is the intensity of the transmitted light beam. This corresponds to a relative change in $f(E)$ of

$$\left(\frac{\Delta f}{f_{\max}}\right)_{\text{noise}} \simeq \frac{1}{2.3(\text{OD})}\frac{\Delta I}{I} \simeq 10^{-5}, \tag{47}$$

where OD is the optical density at the peak of the absorption band and was typically about two.

The above noise level probably arises from two major sources: (1) shot noise; (2) fluctuations in the brightness of the tungsten lamp. Shot noise is due to statistical fluctuations in the number of photoelectrons N ejected from the cathode of the phototube during one integration time constant, which was 1 sec. This fluctuation is given by $\Delta N/N=1/\sqrt{N}$. If all the noise were due to shot noise, this would imply $N=4\times10^8$. Since the quantum efficiency of the cathode was of order 10%, this implies that a photon current of about 4×10^9 photons/sec was incident on the phototube. This may not be unreasonable since the Glan prism used as a polarizer only accepts a small angular spread in the incident beam, reducing the efficiency of the optics.

Since the photon current may have been higher than that estimated above assuming shot noise, other sources of nearly statistical noise may have contributed to the noise level. The most likely are fluctuations in the emissivity of the tungsten filament, the magnitude of which usually varies inversely with the frequency. The frequency of rotation of the polarizer was 20 cps so the frequency of measurement was 40 cps.

These sources of noise could be reduced by using a more intense source, more efficient optics, and going to higher frequencies. The above-stated noise level was small enough, however, to allow the measurements described in this work to be carried out with reasonable accuracy.

The numerical value of $\Delta f_{11}(E)-\Delta f_{\perp}(E)$ can be obtained as follows. Let the amplitude of the 2ω modulation produced by a given stress be $S(E)$. Let the amplitude of the 2ω modulation produced by inserting a polarizer into the beam with no external stress applied be $2S_{100}$ when the photomultiplier voltage is adjusted such that the same average current flows as when the stress is applied. Then the relative change in intensity of transmitted light, $\Delta I/I$ produced by the stress is

$$\Delta I/I=S/S_{100}. \tag{48}$$

The intensity of transmitted light is $I=I_0e^{-\alpha l}$ where I_0 is the incident intensity, l the thickness of the crystal, and α the absorption coefficient. The stress produces a small change in the absorption coefficient and the corresponding change in intensity is given by

$$\begin{aligned} I_{11}-I_{\perp}&=I_0(e^{-(\alpha+\Delta\alpha_{11})l}-e^{-(\alpha+\Delta\alpha_{\perp})l})\\ &=I_0e^{-\alpha l}(l)(\Delta\alpha_{11}-\Delta\alpha_{\perp}) \end{aligned} \tag{49}$$

to first order in $l\Delta\alpha$. The signs of $\Delta\alpha_{11}$ and $\Delta\alpha_{\perp}$ will be regarded as arbitrary at this point. Combining Eqs. (48) and (49)

$$\frac{I_{11}-I_{\perp}}{I}=l(\alpha_{11}(E)-\alpha_{\perp}(E))=\frac{S(E)}{S_{100}}. \tag{50}$$

The absorption shape function is related to the absorption coefficient by[14]

$$f(E)=C\alpha(E)/E, \tag{51}$$

where C is a constant. The value of C is arbitrary for the purposes of evaluating moments since all moments are normalized by dividing by the area of the band. It is convenient to let $C=3$ eV, so that $f(E)\simeq\alpha(E)$ in the range of the spectrum covered in these measurements. Combining Eqs. (49), (50), and (51):

$$f_{11}(E)-f_{\perp}(E)=\frac{3}{E}(\alpha_{11}(E)-\alpha_{\perp}(E))=\frac{3}{E}\frac{1}{l}\frac{S(E)}{S_{100}}. \tag{52}$$

The measurement procedure is as follows. At a given wavelength of light, with the polarizer rotating at frequency ω, and the lock-in amplifier tuned to frequency 2ω, the partial polarization of the incident beam due to the monochromator grating and any other source is cancelled out using a compensator which consists of one or more glass plates which can be oriented at any angle with respect to the incident beam. For angles of incidence other than 90°, glass plates have a smaller

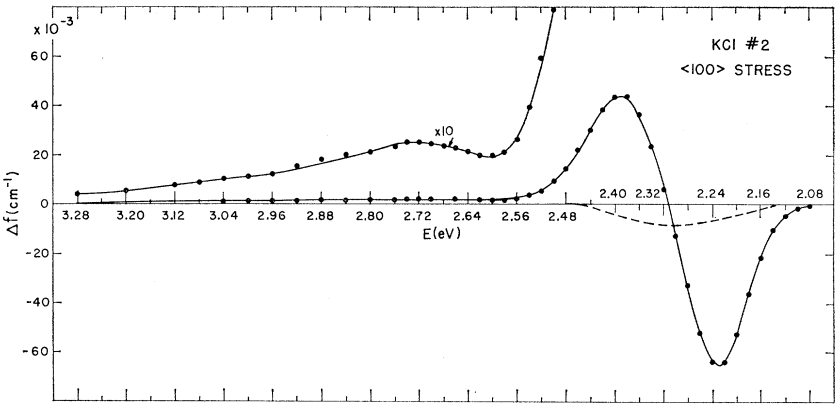

FIG. 3. $\Delta f_{\parallel}(E)-\Delta f_{\perp}(E)$ for KCl using a ⟨100⟩ applied stress. The dashed line shows the area exchange between the F and K bands.

reflection coefficient for light polarized in the plane of incidence than perpendicular to it. Hence they act as partial polarizers. By varying the angle of incidence and rotating the plane of incidence, they can be used to cancel out any amount of polarization of the initial beam up to a maximum which is determined by the number of plates used. The polarization produced by a monochromator depends on the grating spacing, the blaze wavelength, and the wavelength of observation. It was observed to vary over a range of about +30% to −30% in the present work.

With the system optically balanced in this manner, so the lock-in amplifier records zero signal at frequency 2ω, the anode current of the phototube was adjusted to be a standard value, chosen to be 10 μA. Then the stress was applied to the sample, causing it to act as a partial polarizer, and a signal S appeared at a frequency 2ω. Removal of the stress returned the signal to zero. Measurements were made at intervals of 0.02 eV throughout the absorption band.

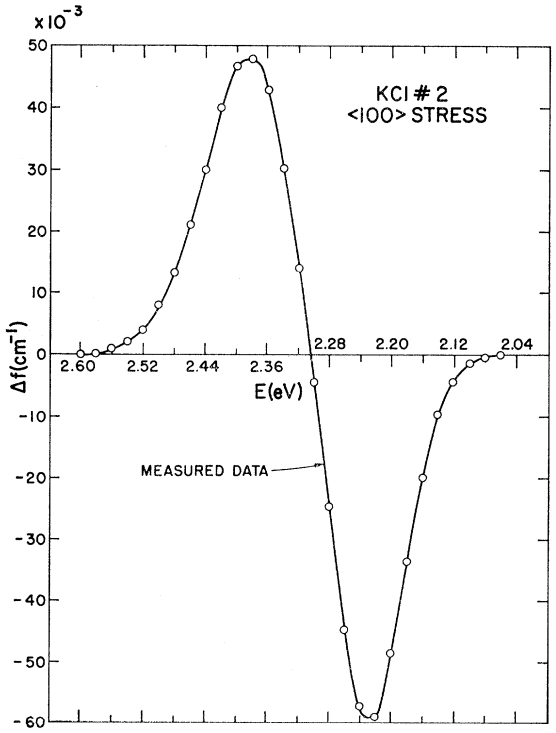

FIG. 4. $\Delta f_{\parallel}(E)-\Delta f_{\perp}(E)$ for KCl using a ⟨100⟩ applied stress corrected for the K band and higher excited states.

B. Data Treatment

Figure 3 shows a graph of $\Delta f_{\parallel}(E)-\Delta f_{\perp}(E)$ for KCl obtained using the procedure described above and Eq. (52). A stress-induced dichroism appears in the K-band region as well as the F-band region. Since we are interested primarily in evaluating parameters of the F band, it is necessary to subtract out the effect of the K band. This can be done using the results of Sec. IV. The K band is assumed to be symmetric about its peak. The K-band stress-induced dichroism has, in the rigid shift approximation, the same shape as the K band, only is shifted to higher energy. This signal can then be extrapolated under the F band and subtracted from the total signal observed.

The remaining signal must still be corrected for the area exchange between the K and F band, and for any possible area exchange between the F band and higher excited states of the F center as well as for the effect of the stress on the ground state. This is accomplished in one step by adding to the remaining dichroism a signal proportional to the F-band shape and of such magnitude that the net area change of the F band is zero (i.e., area of positive lobe equals area of negative lobe). The result is shown in Fig. 4. This is a good approximation of the signal which would have been obtained if the F center had no higher excited states to which optical dipole transitions could occur from the ground state.

It is this corrected result which is used to evaluate the changes in first and third moments. Thus, since the net area change is zero, the energy origin for measure-

TABLE I. Moments of the F band. The first column shows the first moment of the band. The second and third columns indicate the contributions to the second and third moments due to the electron-lattice interaction. The fourth column lists the lattice frequency obtained by Gebhardt and Kühnert (Ref. 19) by measuring the half-width of the absorption band as a function of temperature. The fifth column contains $\langle E^3\rangle_{\mathrm{EL}}{}^{\mathrm{CALC}}$ obtained using Eq. (56).

Sample	$\bar{E}$ (eV)	$\langle E^2\rangle_{\mathrm{EL}}$ (eV^2)	$\langle E^3\rangle_{\mathrm{EL}}$ (eV^3)	ω (sec^{-1})	$\langle E^3\rangle_{\mathrm{EL}}{}^{\mathrm{CALC}}$ (eV^3)
KCl	2.306±0.001	$5.86\pm0.2\times10^{-3}$	$7.7\pm0.4\times10^{-5}$	1.86×10^{13}	5.06×10^{-5}
KBr	2.063±0.001	$6.42\pm0.2\times10^{-3}$	$15.0\pm1.3\times10^{-5}$	1.76×10^{13}	5.10×10^{-5}
KI	1.873±0.001	$4.79\pm0.2\times10^{-3}$	$6.2\pm0.5\times10^{-5}$	1.60×10^{13}	3.22×10^{-5}
NaCl	2.762±0.001	$13.5\ \pm0.4\times10^{-3}$	$24.9\pm1.7\times10^{-5}$	2.76×10^{13}	$21.3\ \times10^{-5}$
RbCl	2.043±0.001	$4.80\pm0.2\times10^{-3}$		1.54×10^{13}	3.07×10^{-5}

ment of $\langle\Delta E\rangle$ is arbitrary, and Eq. (44) can be written

$$\langle\Delta E_{\parallel}\rangle-\langle\Delta E_{\perp}\rangle=\frac{1}{A}\int(\Delta f_{\parallel}(E)-\Delta f_{\perp}(E))(E-\bar{E})dE$$
$$=\frac{1}{A}\sum_n(\Delta f_{\parallel}(n)-\Delta f_{\perp}(n))(n\delta E)(\delta E)$$
$$=\frac{\delta E^2}{A}\sum_n(\Delta f_{\parallel}(n)-\Delta f_{\perp}(n))n, \qquad (53)$$

where n is the number of energy units δE away from the center of gravity of the band. $\delta E=0.02$ eV in these measurements.

In the case of the third-moment change, the number needed is the difference between the rigid-shift third-moment change and the measured result [Eqs. (15) and (16)]. This is obtained as follows. To first order in $\langle\Delta E_{\parallel}\rangle-\langle\Delta E_{\perp}\rangle$, the absorption function change in the rigid-shift case is

$$(\Delta f_{\parallel}(E)-\Delta f_{\perp}(E))_{\mathrm{RS}}=(\partial f/\partial E)(E)(\langle\Delta E_{\parallel}\rangle-\langle\Delta E_{\perp}\rangle). \qquad (54)$$

Hence

$$(\langle\Delta E_{\parallel}{}^3\rangle-\langle\Delta E_{\perp}{}^3\rangle)_{\mathrm{RS}}-(\langle\Delta E_{\parallel}{}^3\rangle-\langle\Delta E_{\perp}{}^3\rangle)_{\mathrm{MEAS}}$$
$$=\frac{1}{A}\int\{(\Delta f_{\parallel}(E)-\Delta f_{\perp}(E))_{\mathrm{RS}}-(\Delta f_{\parallel}(E)-\Delta f_{\perp}(E))_{\mathrm{MEAS}}\}(E-\bar{E})^3dE$$
$$=\frac{\delta E^4}{A}\sum_n\{(\Delta f_{\parallel}(n)-\Delta f_{\perp}(n))_{\mathrm{RS}}-(\Delta f_{\parallel}(n)-\Delta f_{\perp}(n))_{\mathrm{MEAS}}\}n^3. \qquad (55)$$

Equation (53) can be used to evaluate $\langle z|\mathcal{O}_{3a}|z\rangle$ using Eq. (8) and $\langle x|\mathcal{O}_{5a}|y\rangle$ with Eq. (11). Equation (55) can be used to evaluate $\langle E_1{}^2\rangle$, $\langle E_3{}^2\rangle$, and $\langle E_5{}^2\rangle$ using Eqs. (1), (15), and (16).

VI. RESULTS AND DISCUSSION

A. First, Second, and Third Moments of the F Band

Table I shows the measured values of $\bar{E}$, $\langle E^2\rangle_{\mathrm{EL}}$, and $\langle E^3\rangle_{\mathrm{EL}}$ for the F band in five alkali halides at 80±1°K. The third moment of RbCl could not be reliably measured because of a long-wavelength tail which was present on all the observed absorption curves. The uncertainties listed are average deviations of repeated (three or four) measurements of the same quantity. The values of λ quoted by Smith[18] were used to determine $\langle E^2\rangle_{\mathrm{SO}}$ and $\langle E^3\rangle_{\mathrm{SO}}$ in obtaining $\langle E^2\rangle_{\mathrm{EL}}$ and $\langle E^3\rangle_{\mathrm{EL}}$ from $\langle E^2\rangle$ and $\langle E^3\rangle$. This correction is small for both $\langle E^2\rangle$ and $\langle E^3\rangle$ in most cases. Table II shows the values of $\langle E^2\rangle_{\mathrm{SO}}$ and $\langle E^3\rangle_{\mathrm{SO}}$ used in the analysis.

The usual approximation which is made to simplify the moment formulas is to assume that only one-frequency vibrational mode interacts strongly with the F center. The contribution of the electron-lattice interaction to the second and third moments is then given by Eqs. (3) and (4). The temperature dependence of $\langle E^2\rangle_{\mathrm{EL}}$ can be used to obtain a value for ω. With this value of ω the validity of Eqs. (3) and (4) can then be checked by measuring $\langle E^2\rangle_{\mathrm{EL}}$ and $\langle E^3\rangle_{\mathrm{EL}}$ for a given band. The "one-frequency" formulas predict,

$$\langle E^3\rangle_{\mathrm{EL}}{}^{\mathrm{CALC}}=\langle E^2\rangle_{\mathrm{EL}}\frac{\hbar\omega}{\coth(\hbar\omega/2kT)}. \qquad (56)$$

The last two columns of Table I show the values of ω obtained by Gebhardt and Kühnert[19] by measuring the half-width as a function of temperature, and $\langle E^3\rangle_{\mathrm{EL}}{}^{\mathrm{CALC}}$ obtained from the measured second moment with Eq. (56). The average difference between $\langle E^3\rangle_{\mathrm{EL}}$ and $\langle E^3\rangle_{\mathrm{EL}}{}^{\mathrm{CALC}}$ is 40% of $\langle E^3\rangle_{\mathrm{EL}}$. The disagreement is largest for KBr and KI.

TABLE II. Values of the spin-orbit coupling constant, $\langle E^2\rangle_{\mathrm{SO}}$ and $\langle E^3\rangle_{\mathrm{SO}}$ used in the data analysis.

Alkali halide	λ (eV)[a]	$\langle E^2\rangle_{\mathrm{SO}}=\frac{1}{2}\lambda^2$ (eV^2)	$\langle E^3\rangle_{\mathrm{SO}}=-\frac{1}{4}\lambda^3$ (eV^3)
KCl	-6.7×10^{-3}	2.3×10^{-5}	7.5×10^{-8}
KBr	-20.0×10^{-3}	2.0×10^{-4}	2.0×10^{-6}
KI	-38.0×10^{-3}	7.2×10^{-4}	1.4×10^{-5}
NaCl	-5.1×10^{-3}	1.3×10^{-5}	3.0×10^{-8}
RbCl	-16.0×10^{-3}	1.3×10^{-4}	1.0×10^{-6}

[a] Reference 18.

[18] D. Y. Smith, Phys. Rev. 137, A574 (1965).
[19] W. Gebhardt and H. Kühnert, Phys. Letters 11, 15 (1964).

TABLE III. Matrix elements of $\mathcal{A}_1$, $\mathcal{A}_3$, and $\mathcal{A}_5$ obtained in this work and by other authors as indicated.

Sample	$\langle z\|\mathcal{A}_1\|z\rangle$ (eV/kg/mm²) Jacobs[a]	$\langle z\|\mathcal{A}_{3a}\|z\rangle$ (eV/kg/mm²) This work	Gebhardt[b]	$\langle x\|\mathcal{A}_{5a}\|y\rangle$ (eV/kg/mm²) This work	Gebhardt[b]
KCl	$13.6\pm0.5\times10^{-4}$	$6.1\pm0.9\times10^{-4}$	6.6×10^{-4}	$8.8\pm1.2\times10^{-4}$	
KBr	$14.6\pm0.5\times10^{-4}$	$4.4\pm0.6\times10^{-4}$		$6.3\pm0.9\times10^{-4}$	
KI	$17.6\pm0.5\times10^{-4}$	$6.2\pm0.9\times10^{-4}$	7.7×10^{-4}	$9.8\pm1.4\times10^{-4}$	
NaCl	$16.8\pm0.5\times10^{-4}$	$2.4\pm0.4\times10^{-4}$	3.1×10^{-4}	$6.7\pm1.0\times10^{-4}$	7.7×10^{-4}
RbCl	$13.9\pm0.5\times10^{-4}$	$7.0\pm1.0\times10^{-4}$	6.6×10^{-4}	$5.8\pm0.8\times10^{-4}$	

[a] Reference 8.
[b] Reference 20.

The above discrepancy seems significant. The disagreement cannot be attributed to random errors in the measurement since the size of such errors, indicated by the listed uncertainties, is less than the observed differences between $\langle E^3\rangle_{\mathrm{EL}}$ and $\langle E^3\rangle_{\mathrm{EL}}{}^{\mathrm{CALC}}$. It is thought that systematic errors in the data analysis are not large. The method used to extrapolate the K band under the F band is the most likely source of such errors. In each case the K-band absorption was subtracted from the total measured absorption to obtain $f(E)$ for the F band alone. The K band was assumed to be symmetric in extrapolating it under the F band. This extrapolation was made with great care, and adjusted until both $f(E)$ and $df(E)/dE$ for the F band had a reasonable shape. The K band peak position was taken to be that reported by Lüty.[1] Its peak position in NaCl, not measured by Lüty, was found to be 3.10 eV. An estimate of the sensitivity of the moments to the assumed shape of the K band was made by assuming that the K band cut off sharply under the F band. The moments of the F band obtained with this $f(E)$ were calculated for KCl and KBr. The first moment was shifted slightly to higher energy, the second moment was not appreciably changed, and the third moment was reduced by about 10%. Thus the results appear to be fairly insensitive to the assumed shape of the K band.

If more than one frequency is important in the F-center electron-lattice interaction, which is likely to be the case if more than one mode is important in the interaction, then more terms need to be added to Eq. (56). This could be responsible for the lack of agreement between $\langle E^3\rangle_{\mathrm{EL}}$ and $\langle E^3\rangle_{\mathrm{EL}}{}^{\mathrm{CALC}}$. Another source of discrepancy could be anharmonic terms in the lattice potential and nonlinear terms in the electron-lattice interaction.[15]

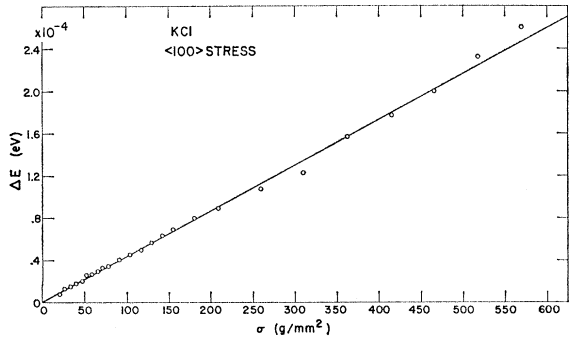

FIG. 5. $\langle\Delta E_{\parallel}\rangle-\langle\Delta E_{\perp}\rangle$ vs applied ⟨100⟩ stress for KCl.

B. First Moment Change Due to Applied Stresses

Figure 5 shows a graph of $\langle\Delta E\rangle$ versus applied stress for KCl. Table III shows the matrix elements of the $\mathcal{A}$'s obtained from the first moment change measurements. The listed uncertainties are average deviations of repeated measurements and do not therefore reflect the size of possible systematic errors in the data analysis, although these errors are thought to be small by an extension of the argument given above.

Gebhardt and Maier[20] have made similar measurements on the F band in alkali halides using additively colored crystals. In analyzing their data, they assumed that the band shifts rigidly upon application of the uniaxial stress and measured the change in absorption only at the half-maximum points of the band. The numbers shown in Table III were obtained from their data after correcting for the fact that the band does not shift rigidly. The correction is typically a factor of 0.85 for the alkali halides included in this study. The essential agreement between Gebhardt's results and those reported in Table III, and the fact that additional measurements carried out on KBr:KH also agreed with those reported here indicates that the results of this type of measurement are independent of the method of sample preparation. This fact is consistent with arguments presented in Ref. 14.

A somewhat more physical way to describe the first-moment changes is to present them in terms of energy change per unit strain. The coupling coefficients defined in this way are:

$$B_1=(c_{11}+2c_{12})\langle z|\,\mathcal{A}_1|z\rangle, \tag{57}$$

$$B_{3a}=\tfrac{3}{2}(c_{11}-c_{12})\langle z|\,\mathcal{A}_{3a}|z\rangle, \tag{58}$$

$$B_{5a}=4c_{44}\langle x|\,\mathcal{A}_{5a}|y\rangle, \tag{59}$$

with similar definitions for B's related to those above by symmetry transformations. The B's are the energy splittings or shifts of the excited state per unit strain of the appropriate symmetry. Note that the B's give the

[20] W. Gebhardt and K. Maier, Phys. Status Solidi 8, 303 (1965).

total energy splittings and not just the perturbation in one of the orbital states. Table IV shows the values of the B's obtained from the measured data.

C. Discussion of the Interaction

The results indicate two qualitative features of interest. First, all three coupling coefficients have the same sign, and second, B_1 is larger than B_3 and B_5.

The significance of the sign of the coupling coefficients can be seen from an estimate of them using the simplest possible model for the electron-lattice interaction, namely the point-ion model. In this approximation the ions in the crystal are replaced by point charges of the appropriate sign, and the interaction with the F-center excited state is purely electrostatic. The breathing mode coupling corresponds to the monopole plus octapole plus higher order terms in the spherical harmonic expansion of the interaction, and the tetragonal and trigonal interactions correspond to the quadrupole plus higher order terms.

In order to simplify this semiquantitative discussion, it is helpful to consider just the ions in the first two shells around the F center. When a $\langle 100\rangle$ stress is applied, positive ions in the first shell are brought closer to the Γ_4 state oriented parallel to the stress, and farther from the state oriented perpendicular to the stress [Fig. 6(a)]. This binds the parallel state more tightly and the perpendicular state more loosely, so that $E_{\parallel}-E_{\perp}<0$. The second shell contributes to the energy change in the same way. To visualize the effect of a trigonal distortion produced by a $\langle 110\rangle$ stress, one must orient the Γ_4 states along the $\langle 110\rangle$ and $\langle 1\bar{1}0\rangle$ directions. In this case, negative charges of the second shell are brought closer to the parallel state and farther from the perpendicular state [Fig. 6(b)]. Thus $E_{\parallel}-E_{\perp}>0$. The first shell contributes to the energy change in the same way. Since the interaction with the first two shells is probably greater than with the rest of the lattice, the point ion approximation predicts B_3 and B_5 will have opposite signs. In actual fact, both B_3 and B_5 have the sign corresponding to a repulsive interaction. Hence, the validity of the point-ion approximation, and in fact, any crystal-field model, is in doubt. A similar discrepancy has been observed by Blume and Orbach.[21]

The discrepancy in the signs of B_3 and B_5, as predicted by the point-ion model, can be removed by including the effects of the finite size of the ions. In addition to the purely electrostatic terms in the interaction, there are terms which arise from the overlap of the F-center wave function with the filled core states of each ion. These terms have their origin in the Pauli principle and are repulsive. The experimental results imply that the net interaction with positive as well as negative ions is repulsive, indicating that the repulsive overlap terms are larger than the attractive electrostatic terms for the positive ions. A recent method for treating such effects is the pseudopotential method.[22,23]

[21] M. Blume and R. Orbach, Phys. Rev. **127**, 1587 (1962).

TABLE IV. Values of B_1, B_{3a}, and B_{5a} obtained using Eqs. (57)–(59) and the matrix elements of $\mathfrak{A}_1$, $\mathfrak{A}_{3a}$, and $\mathfrak{A}_{5a}$ listed in Table III.

Sample	B_1 (eV)	B_{3a} (eV)	B_{5a} (eV)
KCl	8.0±0.2	3.9±0.6	2.3±0.3
KBr	7.2±0.2	2.6±0.4	0.9±0.1
KI	6.9±0.2	3.0±0.4	1.5±0.2
NaCl	12.1±0.2	1.7±0.2	3.5±0.5
RbCl	6.9±0.2	3.7±0.5	1.1±0.1

An approximate test of this interpretation can be made using the present data. It is useful to separate the total interaction into an electrostatic contribution and an overlap contribution. Thus $B_i=B_i^e+B_i^0$, where B_i^e is the coupling due to electrostatic terms and B_i^0 due to overlap terms. According to Gourary and Adrian,[24] the maximum of the excited-state wave function occurs at a distance less than the distance of the first shell for the alkali halides included in this work. Therefore an inward motion of first or second shell ions tends to increase the size of the overlap with those ions thus increasing the energy of the F center electronic state. Figure 6(a) shows that for a tetragonal distortion, the first and second shells contribute to the overlap part of the interaction with opposite signs while the electrostatic terms add. Thus

$$B_3=B_{31}^0-B_{32}^0-(B_{31}^e+B_{32}^e), \tag{60}$$

where B_{31} and B_{32} are the contributions to B_3 due to the first and second shells, respectively. For the trigonal interaction,

$$B_5=B_{52}^0-B_{51}^0+(B_{52}^e+B_{51}^e) \tag{61}$$

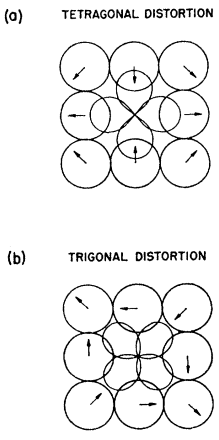

FIG. 6. (a) Displacements of ions in the first and second shells due to a tetragonal distortion. (b) Displacements of ions in the first and second shells due to a trigonal distortion.

[22] M. H. Cohen and V. Heine, Phys. Rev. **122**, 1821 (1961).
[23] B. J. Austin, V. Heine, and L. J. Sham, Phys. Rev. **127**, 276 (1962).
[24] B. S. Gourary and F. J. Adrian, Phys. Rev. **105**, 1180 (1957).

and the breathing interaction

$$B_1=B_{11}^0+B_{12}^0+(B_{12}^e-B_{11}^e). \quad (62)$$

An approximate measure of the size of the overlap terms is the square of the wave function multiplied by the square of the ionic volume. Thus there should exist a consistent variation of B_3^0 and B_5^0 with ionic volume. As the first shell ions increase in size relative to the second shell ions, B_3 should increase and B_5 decrease, according to Eqs. (60) and (61). Figure 7 shows a plot of $B_1/\bar{E}$, $B_{3a}/\bar{E}$, and $B_{5a}/\bar{E}$ versus R_H/R_A where R_H is the halide ionic radius and R_A is the alkali ionic radius. The coupling coefficients have been divided by $\bar{E}$ since most simple model calculations predict $B_i=C\bar{E}$. Although there is considerable scatter in the data, the predicted variation of B_3 and B_5 is consistent with the observed data.

Further measurements extending the range of R_H/R_A to larger values where the variation of B_3 and B_5 appears to increase, would be valuable. Gourary and Adrian's calculations show that for the lithium halides, which have large R_H/R_A values, the maximum of the excited state wave function approaches the first shell position.[24] Since the change in overlap with small change in ionic position for radial displacements is an approximate measure of the slope of the wave function, the value of B_{31}^0 may become very small, and may even change sign if the maximum of the excited wave state function is outside the first shell. Thus one might expect a negative B_3 for some lithium halides.

One possible reason why B_1 is larger than B_3 and B^q also emerges from this model. The largest terms in Eqs. (60) through (62) are the overlap terms. B_3 and B_5 both are proportional to the difference between two overlap terms while B_1 is proportional to the sum of two such terms and is therefore larger. We expect that as the first shell ions become large compared with the second shell ions so that only one shell need be considered, $B_3 \simeq B_1$. This is seen to be the case in Fig. 7.

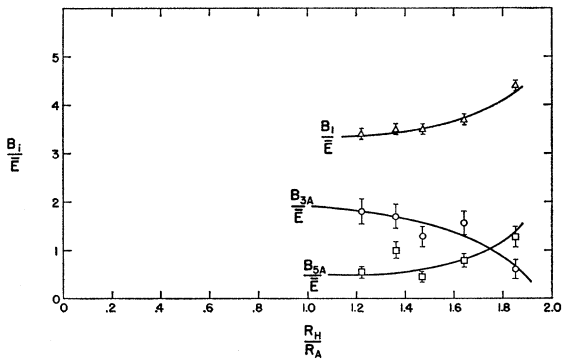

FIG. 7. Electron-lattice coupling coefficients as a function of the ratio of halide to alkali ionic radius.

D. Gebhardt and Maier's Interpretation

Gebhardt and Maier[20] have proposed another explanation for the larger size of B_1. They propose that the local values of the stiffness constants are not the same as the macroscopic values and that the ions in the plane perpendicular to the stress move in toward the vacancy when a stress is applied. This is equivalent to saying that c_{12} has changed sign locally. They evaluate the local values of c_{11} and c_{12} by arguing that since the F center is a perturbation in the lattice of cubic symmetry, it will only change the linear combination of stiffness constants corresponding to a cubic distortion $(c_{11}+2c_{12})$, not affecting the resistance of the lattice to tetragonal $(c_{11}-c_{12})$ or trigonal (c_{44}) distortion.

The following comments about this interpretation seem appropriate. The argument that a cubic perturbation in the lattice can only affect the resistance of the lattice to cubic distortions is incorrect. Let ΔH be the change in the lattice Hamiltonian due to the F center. Then, since ΔH has cubic symmetry, matrix elements of the form $\langle X_l|\Delta H|X_l'\rangle$ are zero unless $|X_l\rangle$ and $|X_l'\rangle$ have the same symmetry. This is as much as can be said from symmetry alone. It is not true that the changes in certain of the stiffness constants will be zero because $|X_l\rangle$ and $|X_l'\rangle$ have the same symmetry. If this were so, then the unperturbed lattice, whose total potential is cubic, would be unstable to noncubic distortions, i.e., have zero values of $c_{11}-c_{12}$ and c_{44}.

Calculations of the stiffness constants show that nearest-neighbor forces do not contribute to c_{12} and c_{44}, that is, c_{12} and c_{44} are both zero if only nearest neighbor forces are considered.[25] The first shell of ions around the F center has been perturbed by the removal of a nearest-neighbor ion. Neglecting the static relaxation of the ions, the above fact argues that c_{12} and c_{44} will be the same in the first shell as in the bulk crystal while c_{11}, which derives much of its value from nearest-neighbro interactions, will be changed. In order to fit the data using only a first shell interaction and changed stiffness constants, even when relaxing the assumption that $c_{11}-c_{12}$ must have its macroscopic value, it is necessary to change c_{11} only slightly, while c_{12} must reverse its sign. This seems unreasonable in view of the above argument.

While it may be unreasonable to attribute all the observed effects to local deviations of the stiffness constants from their bulk values, it nevertheless remains true that such deviations do occur and that their magnitude is unknown. A calculation of the displacements of the ions near a point defect in a solid produced by an applied macroscopic strain would be of great interest.

---

[25] K. S. Krishnan and S. K. Roy, Proc. Roy. Soc. (London) **210**, 481 (1952).

TABLE V. Contributions to the second moment of the F band due to dynamic lattice distortions of Γ_1, Γ_3, Γ_5 symmetries and the spin-orbit interaction.

Sample	$\langle E^2\rangle$	$\langle E_1{}^2\rangle$	$\langle E_3{}^2\rangle$	$\langle E_5{}^2\rangle$	$\langle E_{SO}{}^2\rangle$
KCl	$(0.077\ \text{eV})^2$	$(0.058\pm0.006\ \text{eV})^2$	$(0.032\pm0.003\ \text{eV})^2$	$(0.039\pm0.004\ \text{eV})^2$	$(0.005\ \text{eV})^2$
KBr	$(0.082\ \text{eV})^2$	$(0.073\pm0.007\ \text{eV})^2$	$(0.019\pm0.002\ \text{eV})^2$	$(0.029\pm0.003\ \text{eV})^2$	$(0.014\ \text{eV})^2$
KI	$(0.074\ \text{eV})^2$	$(0.058\pm0.006\ \text{eV})^2$	$(0.028\pm0.003\ \text{eV})^2$	$(0.026\pm0.003\ \text{eV})^2$	$(0.027\ \text{eV})^2$
RbCl	$(0.070\ \text{eV})^2$	$(0.054\pm0.006\ \text{eV})^2$	$(0.029\pm0.003\ \text{eV})^2$	$(0.033\pm0.003\ \text{eV})^2$	$(0.011\ \text{eV})^2$
NaCl	$(0.116\ \text{eV})^2$	$(0.10\ \pm0.016\ \text{eV})^2$	$(0.046\pm0.006\ \text{eV})^2$	$(0.040\pm0.01\ \text{eV})^2$	$(0.004\ \text{eV})^2$

E. Second-Moment Contributions

Figure 8 shows a graph of the corrected values of $\Delta f_{II}(E)-\Delta f_{I}(E)$ in comparison with the rigid-shift result versus the photon energy. The two curves have, of course, the same first moment. It is clear, however, that the rigid-shift result has a larger third moment since this curve is shorter and broader. Using measured curves of this sort and Eqs. (15) and (16), the values of $\langle E_1\rangle$, $\langle E_3\rangle$, and $\langle E_5\rangle$ were obtained. Table V shows the results of the data analysis. An interpretation of the magnitudes of the contributions of the dynamic lattice vibrational modes to the second moment is more difficult than interpreting the coupling to a static stress. This is because more than one kind of lattice mode is involved. The static measurements described above involve the coupling only to long-wavelength acoustic lattice distortions. The effect of shorter wavelengths and the effect of optical phonons can only be calculated if the coupling to a displacement of each ion is known, and if the displacements of the ions due to each mode is known. A qualitative guess at the effects to be expected on the basis of the present rather poor understanding of the interaction mechanism and the lattice dynamics near a point defect will be described.

McCombie and Matthew[26] have calculated the effect on the lattice modes of a point imperfection such as an F center. The first eleven shells were allowed to vibrate in breathing-type modes only, the rest of the lattice remaining fixed. Nearest-neighbor repulsive forces plus full Coulomb interactions were used in the calculation. The F center was treated by including the electrostatic terms in the interaction, but dropping the repulsive term for the first shell. The effect was to enhance greatly the mean-square amplitude of the low-frequency acoustic modes, while reducing the amplitude of optical-mode displacements. This is a result of weakening the effective spring constants of the first shell of ions.

As one goes from one alkali halide to another, it must be the case that this enhancement of acoustic and reduction of optical-mode vibrations decreases as the halide ion becomes small compared with the alkali ion. In the limit of zero halide ion radius, removal of a halide and its replacement by a point charge constitutes no perturbation on the force constants at all. There is a mass change, but this does not affect the even-parity modes with which the F center interacts, because in the case of these modes, the ion at the origin has zero displacement.

Equations (60) through (62) describe the interaction of the F-center excited state with long-wavelength acoustic distortions. In the case of optical distortions, the first and second shells are moving out of phase and the signs in Eqs. (60) through (62) are changed. Hence, for the optical-mode case

$$B_1{}^{op}=B_{11}{}^0-B_{12}{}^0-(B_{11}{}^e-B_{12}{}^e),$$
$$B_3{}^{op}=B_{31}{}^0+B_{32}{}^0-(B_{31}{}^e-B_{32}{}^e),$$
$$B_5{}^{op}=B_{52}{}^0+B_{51}{}^0+(B_{52}{}^e-B_{51}{}^e). \quad (63)$$

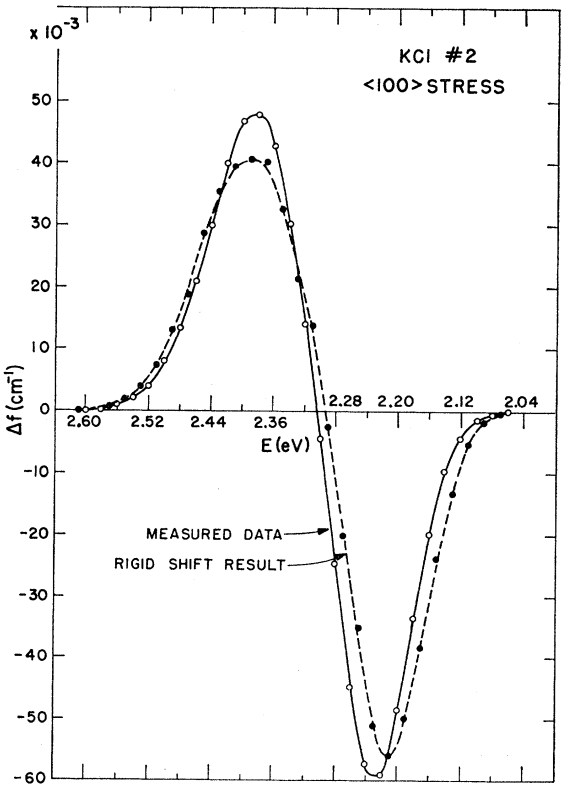

FIG. 8. Corrected $\Delta f_{II}(E)-\Delta f_{I}(E)$ for KCl using a $\langle 100\rangle$ stress in comparison with the rigid-shift result.

[26] C. W. McCombie and J. A. D. Matthew, J. Appl. Phys. Suppl. 33, 359 (1962).

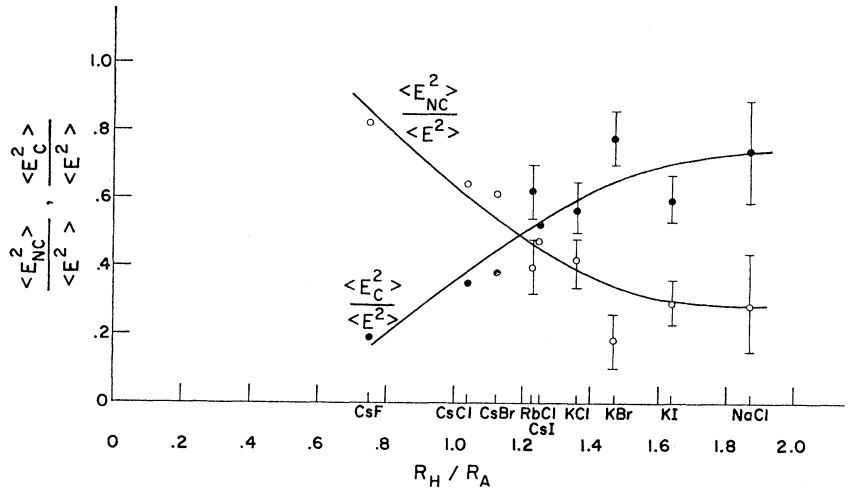

FIG. 9. Fractional cubic and noncubic second moment contributions as a function of the ratio of halide to alkali ionic radius. Cesium halide data taken from Ref. 27.

The coupling to tetragonal and trigonal optical distortions is thus expected to be larger than for the breathing mode, since the overlap terms are larger than the electrostatic terms as demonstrated in Sec. VI C. Hence, the larger the optical-mode vibrational amplitude, the larger will be the noncubic contributions to the second moment. The above argument predicts that as the halide ion becomes small compared with the alkali ion, the relative amount of optical mode vibration increases, and the noncubic second moment contributions increase. Figure 9 shows a plot of

$$\langle E^2\rangle_{NC}/\langle E^2\rangle = (\langle E_3^2\rangle + \langle E_5^2\rangle)/\langle E^2\rangle$$

and $\langle E_1^2\rangle/\langle E^2\rangle$ against R_H/R_A. The data for the cesium halides were obtained from calculations by Moran.[27] The results are clearly consistent with the above arguments. It should be noted, however, that the measurements of the contributions to $\langle E^2\rangle$ described in this paper were carried out at 80°K, while Moran's evaluation was made by fitting the helium temperature absorption curves of the cesium halides. If the noncubic modes have characteristic frequencies which are significantly higher than the cubic modes, most of the increase in second moment between liquid-helium temperature and liquid-nitrogen temperature (typically about a factor of 1.5) may be due to an increase in the breathing mode amplitudes. This effect would exaggerate the difference between Moran's results and the measurements presented in this paper. A measurement of the temperature dependence of the contributions to $\langle E^2\rangle$ would be of interest since it would allow evaluation of the effective breathing, tetragonal, and trigonal mode frequencies.

TABLE VI. Relative change in zeroth moment of the F-K composite band and F band per unit relative change in energy of the F band due to applied static stresses.

Sample	F-K Composite band	F band
	$\frac{\Delta A}{A}\Big/\frac{\Delta E}{E}$	$\frac{\Delta A}{A}\Big/\frac{\Delta E}{E}$
KCl	1.0±0.3	2.4±0.2
KBr	1.4±0.3	5.1±0.3
KI	1.2±0.6	3.4±0.4
RbCl	1.2±0.3	3.3±0.3
NaCl		7.1±0.7

F. Validity of the Condon Approximation

In the Condon approximation, the dipole matrix element of a transition is assumed to be independent of the lattice coordinates. That is, the zeroth moment of the absorption band is independent of Q. One of the quantities measured in this work is the change in area of the F band and F-K composite band upon application of a stress. These measurements allow an estimate of the validity of the Condon approximation. The results are shown in Table VI. The column labeled "F band" appearing in the table shows the relative area change of the F band per unit relative energy change. It includes mixing of the F- and K-band states as described above. The numbers in the column labeled "F-K composite" show the change of the F-K composite band area. This indicates the extent of the mixing of higher excited bound or continuum states into both the F and K states as well as mixing of excited states into the ground state by the applied stress. (The F-K composite area change is not shown for NaCl because the tungsten light source was so weak in the K-band region that the accuracy of the measurements is in doubt.) Thus, for example, in KCl at liquid-nitrogen temperature, the change in transition probability to the F state on going from one half-maximum of the F band to the other due to all effects is

$$\Delta A/A = 2.4(0.2/2.3) \simeq 0.2. \quad (64)$$

[27] P. R. Moran, Phys. Rev. 137, A1016 (1965).

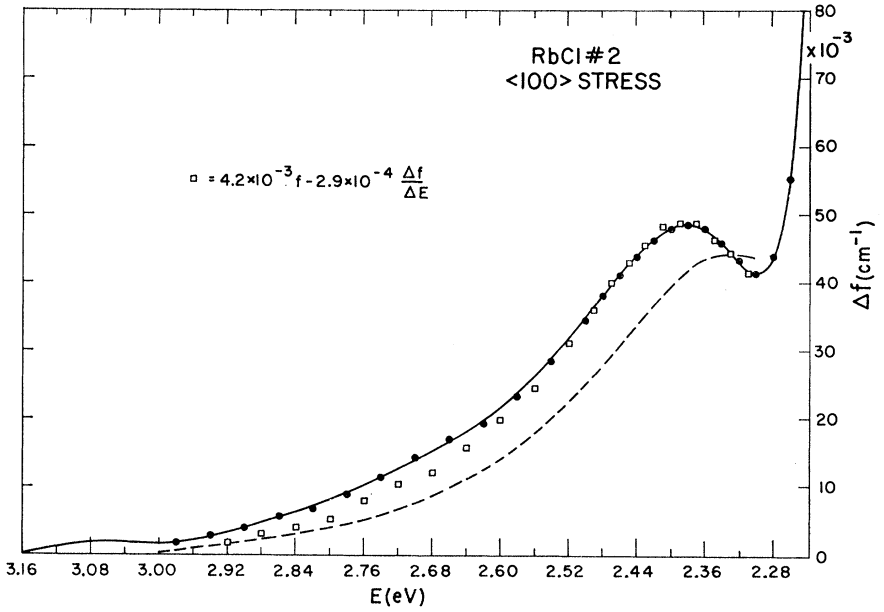

FIG. 10. $\Delta f_{\parallel}(E)-\Delta f_{\perp}(E)$ in the K band region of RbCl for a ⟨100⟩ stress. The dashed line has the shape of the K band and shows the amount of the dichroism which can be attributed to area exchange with the F band.

The results for the F-K composite band are consistent with the calculations of Gourary and Adrian.[24] They found that the oscillator strength of the F band does not vary significantly upon changing the lattice constant. Measurements of the oscillator strength are consistent with the result.[6] Since

$$f_F = C\bar{E}A\,, \tag{65}$$

where f_F is the oscillator strength of the F band (which is the same as the unnormalized first moment) we expect, upon changing the lattice constant,

$$\Delta A/A = -\langle \Delta E\rangle/E. \tag{66}$$

Since Gourary and Adrian did not explicitly include the effect of the K state, their result should be compared with $\Delta A/A$ for the F-K composite band. The agreement is seen to be good.

These results, obtained by applying a static stress, are applicable to the dynamic case only to the extent that long-wavelength acoustic modes are responsible for the broadening of the F band.

Odd-parity lattice vibrations will mix states of opposite parity into the ground and excited states of the F center, changing the area of the band in second order. If the states being mixed are well separated in energy, this effect will occur equally throughout the band since the lattice coordinates of even parity which produce the broadening are independent of the odd-parity lattice coordinates. Thus odd-parity lattice distortions will not change the shape of the band. Even parity distortions cause a change in transition probability which varies linearly with energy if the states being mixed are well separated in energy. Such a change merely shifts the band rigidly away from the state being mixed in and does not cause a change in the shape of the band. Hence, deviations from the Condon approximation do not, in second order, cause significant changes in the shapes of F absorption bands.

G. K Band

Figure 10 presents a graph of $\Delta f_{\parallel}(E)-\Delta f_{\perp}(E)$ in the K-band region of RbCl produced by an [001] applied uniaxial stress. RbCl was chosen for this study since the K band in this crystal is well resolved from the F band and is in a favorable wavelength range. Table VII summarizes the results of these measurements. It is clear that, in agreement with earlier work, the K band acts as though it is due to a transition to a higher excited state of the F center. If it were caused by a separate defect associated with the F center, it is hard to imagine how area exchange could occur between the two bands. The s-state model can be ruled out immediately since it predicts no polarization-dependent first moment change upon application of a uniaxial stress, and such a change is observed. The d-state model predicts slightly different values for $C_{\parallel}-C_{\perp}$ than are observed. The differences are larger than the experi-

TABLE VII. Measured K-band parameters and the values predicted by the s-state model and the d-state model.

	Measured values	s-State model	d-State model
$\langle\Delta E\rangle_K$ / $\langle\Delta E\rangle_F$	⟨100⟩ stress 0.55±0.25	0	?
	⟨110⟩ stress 0.23±0.1	0	?
$C_{\parallel}-C_{\perp}$ / $\langle\Delta E\rangle_F$	⟨100⟩ stress 10.0 ±2.5 eV^{-1}	6 eV^{-1}	6 eV^{-1}
	⟨110⟩ stress 7.4 ±1 eV^{-1}	6 eV^{-1}	6 eV^{-1}

mental uncertainties listed in Table VII, but these uncertainties are average deviations of repeated measurements and do not therefore reflect the size of possible systematic errors. The d-state model cannot be ruled out on the basis of the stress-induced dichroism measurements alone.

The p-state model of the K band does not predict definite values for the changes in the zeroth and first moments, so this model is not severely tested by these measurements. The measurements can, however, be used to evaluate the matrix elements appearing in Eqs. (39), (40), (42), and (43). The results are

$$\frac{\langle\beta_z|\,\mathcal{A}_{3a}|\gamma_z\rangle}{\langle\beta_z|\,\mathcal{A}_{3a}|\beta_z\rangle}=0.55\pm0.14,$$

$$\frac{\langle\gamma_z|\,\mathcal{A}_{3a}|\gamma_z\rangle}{\langle\beta_z|\,\mathcal{A}_{3a}|\beta_z\rangle}=0.55\pm0.25,$$

$$\frac{\langle\beta_x|\,\mathcal{A}_{5a}|\gamma_y\rangle}{\langle\beta_x|\,\mathcal{A}_{5a}|\beta_y\rangle}=0.44\pm0.06,$$

$$\frac{\langle\gamma_x|\,\mathcal{A}_{5a}|\gamma_y\rangle}{\langle\beta_x|\,\mathcal{A}_{5a}|\beta_y\rangle}=0.23\pm0.1. \qquad (67)$$

As discussed in Sec. IV, these values are appropriate also for the many p-state model. The above parameters can be used to estimate the corresponding matrix elements of H_{EL}. Equation (A5) was obtained in this way. These estimates are reliable only to the extent that long-wavelength acoustic lattice distortions interact most strongly with the F and K states, and the interaction strength for cubic distortions is about the same as for noncubic distortions.

VII. CONCLUSION

The method of moments has been used to analyze the results of a measurement of the effect of applied uniaxial stresses on the optical absorption of F centers in five alkali halides. The first-moment change due to applied stresses allows evaluation of the coupling of the F-center excited state to lattice distortions of breathing, tetragonal, and trigonal symmetry. The coupling to each distortion has the same sign, indicating that the repulsive interaction between the F-center electron and both positive and negative ions dominates the interaction. The magnitude of the breathing interaction is larger than that of the tetragonal and trigonal interactions, although the relative sizes of the interactions change considerably on going from one alkali halide to another.

It was found experimentally feasible to measure not only the first moment change, but also the change in the third moment of the band upon application of a uniaxial stress. Third-moment-change measurements allow evaluation of the contributions to the second moment of the F band of dynamic lattice distortions of breathing, tetragonal, and trigonal symmetries. For the five alkali halides studied, the second moment was found to be typically 70% due to breathing interactions, 15% due to tetragonal, and 15% due to trigonal interactions at 80°K. The relative contributions of cubic and noncubic modes to the second moment varies somewhat on going from one alkali halide to another.

Measurement of the change in zeroth moment, or area of the band, upon application of uniaxial stresses allowed an estimate of the validity of the Condon approximation. The relative change in area of the F-K composite band was found to be approximately equal to the negative of the relative change in energy of the band upon application of the perturbation. This result is consistent with the calculations of Gourary and Adrian.

Measurements of the stress-induced dichroism in the K-band region were compared with calculations based on three simple models of the K band. It was found that the results are not consistent with the assumption that the K band is caused by transitions to a Γ_1 (s-like) state made partially allowed by admixture of some Γ_{4u} (p-like) F-band state by odd-parity lattice vibrations. The Γ_3 and Γ_5 (d-like) model and the Γ_4 (p-like) model are both consistent with the results of the measurements. Calculations of the temperature dependence of the zeroth moment of the K band using the d-state and s-state models show that these models predict a strong temperature dependence of this quantity, which is not observed. The temperature dependence of the zeroth and first moments of the band using a p-state model are consistent with the observed temperature invariance of the high-energy side of the K band. The anomalous shape of the band can be explained by postulating that many p-like states contribute to the absorption in the K-band region.

ACKNOWLEDGMENTS

The author wishes to thank his thesis advisor, Professor W. D. Compton, for his continual help and advice throughout the progress of this work. Thanks are due to Professor C. P. Slichter, without whose assistance and interest the measurements described in this paper would not have been fully understood. The author acknowledges the great help of Dr. C. H. Henry, with whom he worked for many months on theoretical and experimental problems, and Professor M. V. Klein, with whom he discussed the lattice-dynamical aspects of the work. R. E. Hetrick deserves thanks for assistance in carrying out some of the measurements in the later stages of the work. Innumerable useful discussions with Dr. D. Y. Smith, Dr. W. B. Fowler, Dr. T. Timusk, and Dr. P. R. Moran are gratefully acknowledged.

APPENDIX: TEMPERATURE DEPENDENCE OF THE K BAND

There are at least two puzzling features of the K band which any model must explain. One is the anomalous shape of the band, its high-energy side being closer to an exponential function of energy than the usual Gaussian shape which characterizes most color-center bands, and the other is that the peak position and width of the band appear to be independent of the temperature.[1] It is desirable to test the above discussed models of the K band further by seeing whether any of them can explain these observed facts.

A. s- State and d-State Models

The s- and d-state models of the K band are similar in that the area of the K band in each case is proportional to a term of the form

$$A_K \sim \sum_d \frac{|\langle z|H_{\mathrm{EL}}|d\rangle|^2}{\Delta^2} = \sum_{n\mu m d} \frac{|\langle z|V_{n\mu m}|d\rangle|^2}{\Delta^2}\langle Q_{n\mu m}{}^2\rangle = \sum_{n\mu m d} \frac{|\langle z|V_{n\mu m}|d\rangle|^2}{\Delta^2}\frac{\hbar}{2M_{nm}\omega_{nm}}\coth\frac{\hbar\omega_{nm}}{2kT}. \quad \text{(A1)}$$

Thus the area of the K band should be strongly temperature-dependent. Examples of this kind of behavior are well known in the field of molecular spectra.[28,29] The minimum temperature dependence of A_K can be obtained by inserting the highest possible value for ω_{nm} into Eq. (A1). For RbCl this value is the highest frequency of the longitudinal optical mode. Above $\omega \simeq 3\times 10^{13}$ sec^{-1}, the density of states of the longitudinal optical mode falls off rapidly.[30] Using this frequency, one finds the minimum increase in the area of the K band for both the s- and d-state models is a factor of 1.5 upon warming from 0 to 80°K, and nearly a factor of 3 upon warming from 0 to 300°K. These results are not consistent with the observed facts.[1]

B. p- and Many-p-State Models

It does not appear that the Γ_4-state model of the band is consistent with the observed facts either. Such a model predicts a nearly Gaussian band which should broaden with temperature changes. The observed shape alone is enough to disqualify this model. A modification of the Γ_4-state model may, however, be able to explain the observed facts.

Mott and Gurney[2] have suggested that the absorption in the K-band region is due to the hydrogenic series of p-like states approaching the series limit at the conduction band edge. This argument is strengthened somewhat by the fact that the relative size of the K-band and F-band oscillator strengths is about the same as that of the $2s$ and $2p$ transition and the $2s$ to all-higher (bound and continuum) states transitions in atomic lithium.[31] This fact is relevant only to the extent that the F-center wave function is a linear combination of alkali-atom wave functions.

The shape of the K band according to this model is determined by the distribution of excited p-like states in energy, the variation of oscillator strength with energy, and the broadening of the levels due to the electron-lattice interaction. Smith has carried out some preliminary calculations of the K-band shape using this model, with promising results.[3] Spinolo[32] has found the many-p-state model to be consistent with the photoconductivity in the K-band region as observed by Crandall and Mikkor.[33]

As mentioned above, the width and peak position of the K band appear to be independent of temperature. The second moment of the K band using the above model can be written

$$\langle E^2\rangle_K = \sum_i \{\langle E^2\rangle_i + (A_i/A_K)(E_i - \bar{E}_K)^2\}, \quad \text{(A2)}$$

where $\langle E^2\rangle_i$ is the second moment of the ith p-like state measured about its own center of gravity, and A_i and E_i are the zeroth and first moments of the ith p-like state, respectively. A_K and $\bar{E}_K$ are the zeroth and first moments of the composite K band. When the temperature changes, the first term in Eq. (A2) will change, while the second term remains constant in the approximation that the distribution in energy of the excited p-like states shifts rigidly with changes in temperature. Unless the relative size of the two terms is known, it is impossible to determine the change in $\langle E^2\rangle_K$ and hence in the width of the K band. If the first term is small compared with the second term, there may be little or no observable change in the K-band width with temperature.

Dynamic lattice distortions cause a mixing of the F-band state and each of the higher p-like states. Let $|\gamma\rangle$ be a K-band Γ_4 state and $|\beta\rangle$ the F band Γ_4

---

[28] C. J. Ballhausen, *Introduction to Ligand Field Theory* (McGraw-Hill Book Company, Inc., New York, 1962), p. 185.

[29] For an example of this type of phenomenon involving silver-doped alkali halides, see R. S. Knox, J. Phys. Soc. Jap. 18, Suppl. II, 218 (1963).

[30] A. M. Karo, J. Chem. Phys. 33, 7 (1960).

[31] F. Seitz, *The Modern Theory of Solids* (McGraw-Hill Book Company, Inc., New York, 1940), p. 645.

[32] G. Spinolo (private communication).

[33] R. Crandall and M. Mikkor (to be published).

state. To second order in H_{EL}, the states $|\gamma\rangle$ are written

$$|\gamma_2\rangle=|\gamma\rangle\left(1-\frac{1}{2}\sum_\beta\frac{|\langle\beta|H_{\mathrm{EL}}|\gamma\rangle|^2}{\Delta^2}\right)+\sum_\beta|\beta\rangle\frac{\langle\beta|H_{\mathrm{EL}}|\gamma\rangle}{\Delta}+\sum_\beta|\beta\rangle\frac{\langle\beta|H_{\mathrm{EL}}|\gamma\rangle}{\Delta^2}\times\{\langle\beta|H_{\mathrm{EL}}|\beta\rangle-\langle\gamma|H_{\mathrm{EL}}|\gamma\rangle\}. \quad \text{(A3)}$$

Using this corrected wave function, the zeroth and first moments of the K band can be calculated. Let A_{K0} denote the area of the K band to first order in H_{EL} and A_K the area calculated to second order. The result is independent of the polarization of the light, so to simplify the expressions, the formulas will be written for light polarized in the x direction. $|\beta_x\rangle$ and $|\gamma_x\rangle$ denote the F- and K-band states which absorb light polarized in the x direction. We obtain

$$\frac{A_K}{A_{K0}}=1-\sum_\beta\frac{|\langle\beta|H_{\mathrm{EL}}|\gamma_x\rangle|^2}{\Delta^2}+\frac{A_{F0}}{A_{K0}}\sum_\gamma\frac{|\langle\beta_x|H_{\mathrm{EL}}|\gamma\rangle|^2}{\Delta^2}+2\left(\frac{A_{F0}}{A_{K0}}\right)^{1/2}\sum_{\beta\gamma}\frac{\langle\gamma_x|H_{\mathrm{EL}}|\beta_x\rangle}{\Delta^2}\times\{\langle\beta_x|H_{\mathrm{EL}}|\beta\rangle-\langle\gamma_x|H_{\mathrm{EL}}|\gamma\rangle\}. \quad \text{(A4)}$$

A numerical estimate can be made of the matrix elements of H_{EL} using the measured values of the matrix elements of H_p as described in Sec. VI G. The results are

$$\langle\gamma|H_{\mathrm{EL}}|\beta\rangle\simeq 0.48\langle\beta|H_{\mathrm{EL}}|\beta\rangle,\qquad \langle\gamma|H_{\mathrm{EL}}|\gamma\rangle\simeq 0.40\langle\beta|H_{\mathrm{EL}}|\beta\rangle. \quad \text{(A5)}$$

So, approximately

$$\frac{A_K}{A_{K0}}=1+0.23\frac{\langle E^2\rangle_F}{\Delta^2}\left\{\frac{A_{F0}}{A_{K0}}+3.0\left(\frac{A_{F0}}{A_{K0}}\right)^{1/2}-1\right\}, \quad \text{(A6)}$$

where the fact has been used that

$$\sum_\beta|\langle\beta|H_{\mathrm{EL}}|\gamma_x\rangle|^2=\sum_\gamma|\langle\beta_x|H_{\mathrm{EL}}|\gamma\rangle|^2.$$

Upon warming from helium temperature to room temperature, $\langle E^2\rangle_F$ increases by approximately 10^{-2} eV^2. Using $\Delta=0.33$ eV and $A_{F0}/A_{K0}\simeq 9$, the change in zeroth moment of the K band due to this temperature change is

$$\Delta A_K/A_K\simeq 0.39. \quad \text{(A7)}$$

Thus the area of the band increases by 39% upon warming from 0 to 300°K.

The first moment of the K band to second order in H_{EL} is

$$\bar{E}_K=\frac{1}{A_K}\left\{\bar{E}_{K0}-2A_{K0}\bar{E}_{K0}\sum_\gamma\frac{|\langle\beta_x|H_{\mathrm{EL}}|\gamma\rangle|^2}{\Delta^2}+A_{F0}\bar{E}_{K0}\sum_\gamma\frac{|\langle\beta_x|H_{\mathrm{EL}}|\gamma\rangle|^2}{\Delta^2}+A_{K0}\bar{E}_F\sum_\gamma\frac{|\langle\beta_x|H_{\mathrm{EL}}|\gamma\rangle|^2}{\Delta^2}+2(A_{F0}A_{K0})^{1/2}\bar{E}_{K0}\sum_{\beta\gamma}\frac{\langle\beta_x|H_{\mathrm{EL}}|\gamma_x\rangle}{\Delta^2}\{\langle\beta_x|H_{\mathrm{EL}}|\beta\rangle-\langle\gamma_x|H_{\mathrm{EL}}|\gamma\rangle\}+2A_{K0}\sum_\gamma\frac{|\langle\beta_x|H_{\mathrm{EL}}|\gamma\rangle|^2}{\Delta}+2(A_{F0}A_{K0})^{1/2}\sum_\beta\frac{|\langle\beta|H_{\mathrm{EL}}|\gamma\rangle|^2}{\Delta}\right\}. \quad \text{(A8)}$$

Using Eq. (A4) for A_K,

$$\bar{E}_K=\bar{E}_{K0}+\sum_\gamma\frac{|\langle\beta_x|H_{\mathrm{EL}}|\gamma\rangle|^2}{\Delta}\left(1+2\left(\frac{A_{F0}}{A_{K0}}\right)^{1/2}\right). \quad \text{(A9)}$$

Thus, the change in $\bar{E}_K$ due to second order terms in H_{EL} is, approximately

$$\bar{E}_K-\bar{E}_{K0}=(0.23)(\langle E^2\rangle_F/\Delta)(1+2(A_{F0}/A_{K0})^{1/2}). \quad \text{(A10)}$$

Upon warming from 0 to 300°K, this change is

$$\bar{E}_K-\bar{E}_{K0}=0.04\text{ eV}. \quad \text{(A11)}$$

This correction is due to the energy repulsion of the K and F states caused by H_{EL}. The K band is shifted to higher energy, and the F band shifted to lower energy by a smaller amount so the center of gravity of the two bands remains fixed.

Jacobs[8] has argued that the temperature shift of the peak position of the F band is due mostly to thermal expansion of the solid. Upon warming from 0 to 300°K, the F band in RbCl shifts about 0.10 eV to the red. In order to estimate how much the K band shifts due to thermal expansion, it is necessary to know the coupling of the K state to lattice distortions of cubic symmetry. Since no hydrostatic pressure data is available, this must be estimated. Using the arguments presented above in Sec. VI B, we expect the cubic coupling to be even larger compared with the noncubic

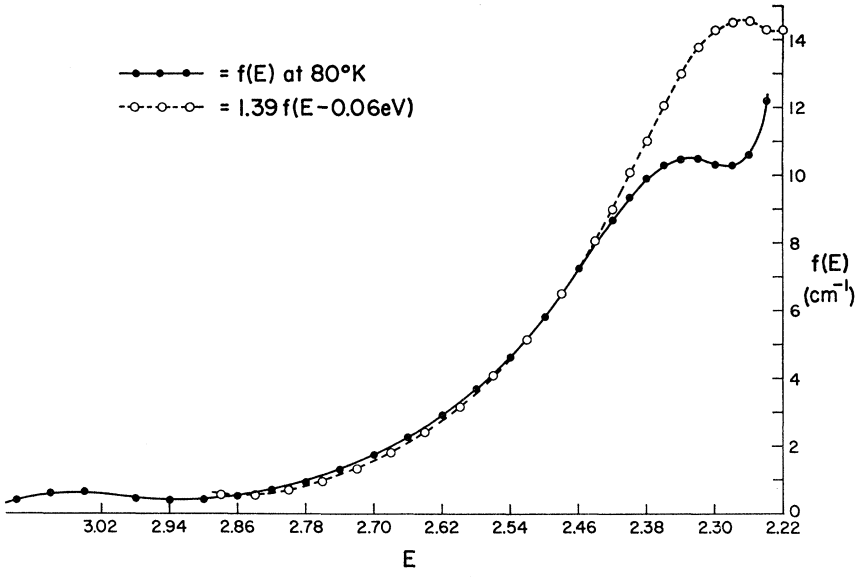

FIG. 11. The effect of a temperature change of 300°K on the absorption in the K band region of RbCl using the parameters described in the text.

for the K state than for the F state since the overlap of the wave function with the second and higher shells is larger relative to the first shell overlap for the K state than for the F state. Thus from Table VII, we expect $\langle\Delta E\rangle_K > \frac{1}{2}\langle\Delta E\rangle_F$ due to temperature changes for an isolated K state. Since no reliable numbers are available, it is necessary to take the approach of choosing a value for $\langle\Delta E\rangle_K$ which best fits the experimentally observed temperature dependence of the K band, to see if the value obtained in this way is reasonable. This value is $\langle\Delta E\rangle_K \simeq \langle\Delta E\rangle_F$, i.e., the isolated K-band peak shifts as much as the F-band peak due to cubic distortions. If this coupling is used, then the effect of a temperature increase from 0 to 300°K is to shift the band 0.10 eV to the red due to thermal expansion and 0.04 eV to the blue due to repulsion by the F-band state for a net shift of 0.06 eV to the red, with an increase in the band height of 39%. Figure 11 shows the effect of a growth and shift of this amount. The band appears unchanged except near the peak. In making measurements of the K-band absorption as a function of temperature, the region of the peak is obscured at high temperatures by the broadened F band. Thus this calculation appears to be consistent with the observed data.[1]

The principal sources of error in this calculation are: (a) neglect of broadening of the K band due to either term in Eq. (A2); (b) neglect of mixing of the K and F states with other excited bound and continuum states by H_{EL}; (c) neglect of mixing of the ground state with excited states by H_{EL}; (d) assumption of a constant value for $\langle\gamma|H_{\mathrm{EL}}|\beta\rangle/(E_\beta - E_\gamma)$; (e) the estimates of the matrix elements in Eq. (A5); and (f) the estimate of the coupling of the isolated K band to lattice distortions of cubic symmetry. Since errors due to the combined effect of these approximations may be significant, this calculation merely indicates that the many-p-state model of the K band is probably consistent with the known facts about the K band.